APPLICATION OF NEURAL NETWORK FOR TRANSFORMER PROTECTION

A thesis submitted in partial fulfilment of the requirements for award of the Degree of

MASTER OF TECHNOLOGY

IN

Power Control & Drives

BY

SANTOSH KUMAR NANDA

Under the Guidance of

Prof. Gopalakrishna Srungavarapu

Department of Electrical Engineering

National Institute Technology,

Rourkela-769008

APPLICATION OF NEURAL NETWORK FOR TRANSFORMER PROTECTION

A thesis submitted in partial fulfilment of the requirements for award of the Degree of

MASTER OF TECHNOLOGY

IN

Power Control & Drives
BY

SANTOSH KUMAR NANDA
Roll no- 211EE2135

Under the Guidance of

Prof. Gopalakrishna Srungavarapu

Department of Electrical Engineering

National Institute Technology,

Rourkela-769008

Dedicated to Lisa

The spring of love in my life

CERTIFICATE

This is to certify that the dissertation entitled "*Application Of Neural Network For Transformer Protection*" being submitted by **Santosh Kumar Nanda**, **Roll No. 211ee2135**, in partial fulfillment of the requirements for the award of degree of *Master Of Technology In Electrical Engineering (Power Control & Drives)* to the *National Institute of Technology, Rourkela*, is a bonafide record of work carried out by him under my guidance and supervision.

(Dr. Gopalakrishna Srungavarapu)
Assistant Professor

Date: Department of Electrical Engineering

Place: **NIT Rourkela**

The thesis is recommended for the award of M.Tech.Degree

DECLARATION

I hereby declare that the investigation carried out in the thesis has been carried out by me. The work is original and has not been submitted earlier as a whole or in part for a degree/diploma at this or any other institution / University.

Santosh Kumar Nanda

Acknowledgement

I am mainly indebted to my guide Dr. S. Gopalakrishna who acts like a pole star for me during my voyage in the research by his infusion, support, encouragement and care. I express my deep regard to him for the successful completion of this work. The blessing, help and guidance given by him from time to time made it possible for me to complete the work in stipulated time. His heart being a great ocean of compassion and love not only created friendly environment during my work with him but also enlightened my soul.

I am thankful to Prof. Anup Kumar Panda, Head of the Department of Electrical Engineering, National Institute of Technology, Rourkela, for providing me facilities to carry out my thesis work in the Department of Electrical Engineering.

I express my sincere gratitude to all the faculty members of Department of Electrical Engineering, NIT Rourkela for their affection and support.

I am thankful to all the staff members of Department of Electrical Engineering, National Institute of Technology, Rourkela for their support.

I render my respect to all my family members and my well-wishers for giving me mental support and inspiration for carrying out my research work.

I thank all my friends who have extended their cooperation and suggestions at various steps in completion of this thesis.

Santosh Kumar Nanda

ABSTRACT

The demand for a reliable supply of electrical energy for the exigency of modern world in each and every field has increased considerably requiring nearly a no-fault operation of power systems. The crucial objective is to mitigate the frequency and duration of unwanted outages related to power transformer puts a high pointed demand on power transformer protective relays to operate immaculately and capriciously. The high pointed demand includes the requirements of dependability associated with no false tripping, and operating speed with short fault detection and clearing time. The second harmonic restrain principle is widely used in industrial application for many years, which uses discrete Fourier transform (DFT) often encounters some problems such as long restrain time and inability to discriminate internal fault from magnetizing inrush condition. Hence, artificial neural network (ANN), a powerful tool for artificial intelligence (AI), which has the ability to mimic and automate the knowledge, has been proposed for detection and classification of faults from normal and inrush condition. The wavelet transform(WT) which has the ability to extract information from transient signals in both time and frequency domain simultaneously is used for the analysis of power transformer transient phenomena in various conditions. All the above mentioned conditions of power transformer to be analysed in a power system are modelled in MATLAB/SIMULINK environment. Secondly the WT is applied to decompose the different current signals of the power transformer into a series of detailed wavelet components. The statistical features of the wavelet components are calculated and are used to train a multilayer feed forward neural network designed using back propagation algorithm to discriminate various conditions. The ANN is tested by varying the hidden layers, number of nodes in the hidden layer, learning rate and momentum factor, and the best suitable architecture of ANN is selected having least mean square error during training. The ANN model is implemented in LabVIEW environment. The results obtained are accurate and encouraging.

Table of contents

List of figures

List of tables

ACRONYMS

EHV	Extra high voltage
DFT	Discrete Fourier transform
FFT	Fast Fourier transform
WT	Wavelet transform
AI	Artificial intelligence
ANN	Artificial neural network
OE	Over excitation
EF	External fault
$V(t)$	Supply voltage
V_m	Maximum value of supply voltage
ω	Angular frequency
$i(t)$	Current in the primary winding
R	Resistance of transformer primary winding
$\Phi(t)$	Flux in the transformer core
N	No. of turns in the primary winding
Φ_m	Maximum value of flux
H_0	High pass filter
G_0	Low pass filter
σ	Steepness constant
$x_1, x_2, \ldots x_m$	Input signal
W_{k_i}	Synaptic weight of the neural network
U_k	Linear combined output due to input signal
b_k	Bias
$\varphi(.)$	Activation function
Y_k	Output signal of the neuron
X	Input training vector
t	Output target vector
δ_k	Error at output unit Y_k
δ_j	Error at hidden unit Z_j
n	Learning rate
V_{nj}	Bias on hidden unit j
Z_j	Hidden unit j
W_{ok}	Bias on output unit k
m	Momentum factor
$d_1[n]$	Detail coefficient of first level decomposition
$d_2[n]$	Detail coefficient of second level decomposition
$d_3[n]$	Detail coefficient of third level decomposition
$d_4[n]$	Detail coefficient of fourth level decomposition
$a_3[n]$	Approximate coefficient of fifth level decomposition

CHAPTER – 1

INTRODUCTION

1.1 General

The demand for a reliable supply of electrical energy for the exigency of modern world in each and every field has increased considerably requiring nearly a no-fault operation of power systems. Power transformers are a class of very expensive and vital components of electric power systems. The crucial objective to mitigate the frequency and duration of unwanted outages related to power transformer puts a high pointed demand on power transformer protective relays to operate immaculately and capriciously. The high pointed demand includes the requirements of dependability associated with no false tripping, and operating speed with short fault detection and clearing time.

Protection of large power transformers is a very challenging problem in power system relaying. The protective system include devices that recognize the existence of a fault, indicates its location and class, detect some other abnormal fault like operating conditions and starts the inceptive steps of opening of circuit breakers to disconnect the faulty equipment of the power system.

Recent development in the field of digital electronics and signal processing made it possible to build microprocessor based relays which provide a viable alternative to the electromechanical and solid state relays. Microprocessor based relays use software for interpreting signals and implementing logic. With the advent of microprocessor various digital algorithms have been developed and successfully implemented for power transformer protection.

There are problems which are peculiar to transformer, which are not encountered in other items of power system. One of the major problem is the large magnetising inrush

current, whose magnitude can be as high as internal fault current and may cause false tripping of the breaker. A common differential relay operating on the basis of measurement and evaluation of currents at both sides of the transformer can't avoid the trip signal during inrush condition.

Since the transformer inrush current is rich in second harmonic component therefore to avoid the needless trip by inrush current harmonic restraint logic together with differential logic is used in most of the fault detection algorithm in the digital differential protection of power transformer. These methods utilize the fact that the ratio of the second harmonic to fundamental component of differential current under inrush conditions is greater in comparison to that under fault conditions.

1.2 Motivation

Although the second harmonic restraint principle is widely used in industrial application for many years, it often encounters some problems such as long restrain time when a long line is connected to the protected transformer. In the traditional method the altitude of second harmonic and fundamental are computed by discrete Fourier transform (DFT) and the ratio is used to judge whether the current is inrush or internal fault one. But it is well known that DFT is not accurate if the current is contaminated by harmonics that are not integer multiples of the fundamental, especially when the computation window is very short and DFT only accounts for frequency analysis but does not give information in the time domain. While DFT assumes a periodic signal, inrush current and fault currents are non-stationary signals.

Mechanical forces build up under large inrush current condition within the transformer coils compared to those occurring at short circuit which is the reason for damage of large power transformer. Large inrush currents also affect the power quality by adding harmonics. Also the presence of large quantity of harmonics in the inrush current can cause damage to power factor correction capacitor by exciting resonant overvoltage. Hence steps are taken to mitigate the transformer inrush current by controlled switching and use of low loss amorphous core materials in modern power transformer that produce inrush current with low second and fifth harmonic contents

Second harmonic component can also be present during internal faults due to saturation of current transformers, parallel capacitances or the distributed capacitances of

long EHV transmission line which are connected to transformer. The second harmonic in these situations might be greater than second harmonic in inrush current.

Hence the above shortcomings of the harmonic restraint differential protection scheme used for power transformer protection conventionally creates a plot for the development of new algorithm based on advanced digital signal processing techniques and artificial intelligence approaches to power system protection which can improve discrimination between normal, inrush, over excitation and fault conditions and facilitate faster, more secure and dependable protection for power transformers.

Since inrush and fault currents are non-stationary signals and these fast electromagnetic transients are non-periodic containing both high frequency oscillations and localized impulses superimposed on the power frequency and its harmonics therefore wavelet transform is a suitable method for the feature extraction from the waveforms of power transformer under various situations. Neural networks on the other hand being a good classifier is used to classify and discriminate the various conditions. The extracted features acts as the input to the neural networks and output of the neural networks are fed to the digital relay to take decision for the breaker operation. Keeping the above idea in mind the following objectives have been set.

1.3 Thesis objective:

- Study of a power transformer in a power system in MATLAB/SIMULINK environment for the following cases.
    1. Normal operation
    2. Inrush condition
    3. Internal fault condition
        I. Single line to ground fault
        II. Double line to ground fault
        III. Three phase line to ground fault
        IV. Line to line fault
        V. Three phase short circuit
    4. Over excitation condition
    5. External fault condition
- Statistical feature extraction from the waveforms of all the above cases using WT.

- Normalization of the data obtained from wavelet transform and principal component analysis.
- Construction of artificial neural network (ANN) to classify all the situations.
- Training and testing of modelled ANN.
- Selection of best architecture of ANN.
- Study of performance of ANN for a set of test data to classify all the conditions.
- Implementation of the present algorithm in LabVIEW.

1.4 Literature survey:

In the literature of power transformer protection, the key issue lies in discriminating between transformer magnetizing inrush current and internal fault current. It is natural that relay should be initiated in response to internal fault but not to inrush current or over-excitation/external fault current [4].

Early methods were based on desensitizing or delaying the relay to overcome the transients [5]. These methods are unsatisfactory since the transformer may be exposed for a long unprotected time. Yet another method based on the second harmonic content with respect to the fundamental one was introduced, known as harmonic restraint differential protection [8], which improved security and dependability was appreciated. However, some researchers have reported the existence of a significant amount of the second harmonic in some winding faults [7, 8]. In addition, the new generations of power transformers use of low-loss amorphous material in their core, which can produce inrush current with lower harmonic contents and higher magnitudes [8]. In such cases, some authors have modified the ratio of second harmonic to fundamental restraining criterion by using other ratios defined at a higher frequency [9]. While other researchers proposed wave comparison and error estimation method [10], fuzzy logic based techniques [7], principal component analysis [11], and correlation analysis method [12] to discriminate internal fault condition from non-fault condition.

Power flow through the transformer is also be used as an index to detect inrush current. Zero average power during energisation and large power consumption during internal fault was the identification key in [13]. However, all the preceding approaches share the same feature, i.e. they depend on a single index. Furthermore, to choose a proper threshold for discrimination is not easy.

4

Artificial Neural Networks (ANN) is extremely used particularly in the field of power system protection since 1994 as this problem is subclass of pattern recognition of current waveforms. It is to be noted that ANNs were primarily used in different areas such as pattern recognition, image processing, load forecasting, power quality analysis, and data compression. The main advantage of the ANN method over the conventional method is the non-algorithmic parallel distributed architecture for information processing and inherent ability to take intelligent decision. In recent years, few works which investigate the feasibility of using ANN for power transformer differential protection has also been reported [14–21].However, the ANNs in these existing studies are specific to particular transformer systems, and would have to be retrained again for other systems. Moreover, the employed feature extraction techniques are based on either time or frequency domain signals, or not both time and frequency features of the signal; this is very important for accurately distinguishing between an internal fault and inrush current.

The wavelet transform is a relatively new and powerful tool in the analysis of the power transformer transient phenomenon because of its ability to extract information from the transient signals simultaneously in the time and frequency domain, rather than conventional Fourier Transform which can only give the information in the frequency domain. Recently, the wavelet transforms have been applied to analyse the power system transients [22], power quality [23], as well as fault location and detection problems [24]. In reference [25], the wavelet transform for analysing the transient phenomena in a power transformer under conditions of faults and magnetizing inrush currents was presented, and simulated results have shown that it is possible to use certain wavelet components to discriminate between internal faults and magnetizing inrush currents.

1.5 Organisation of the thesis:

The thesis structure is organised as follows:

CHAPTER 1 gives a general over-view of need of power transformer protection, detection and classification of fault conditions, demerits of conventional algorithm, a scope for application of ANN as a classifier, advantage of WT, thesis objective and literature survey.

CHAPTER 2 covers a brief discussion on transformer magnetizing inrush current and differential protection scheme.

CHAPTER 3 deals with brief review of ANN and Wavelet transform.

CHAPTER 4 covers the DFT analysis and finds the scope for advanced signal processing techniques.

CHAPTER 5 covers the wavelet analysis of simulated transient current signals.

CHAPTER 6 discusses the performance of ANN and LabVIEW implementation.

CHAPTER 7 gives general conclusion and scope for future work followed by references and appendices.

CHAPTER – 2

TRANSFORMER PROTECTION

AND

INRUSH CURRENT

2.1 General

Inrush current is defined as the maximum, instantaneous input current drawn by an electrical device during starting or turn on. During energization of power transformer a transient current up to 2 to 5 times flow for several cycles and is known as magnetic inrush. This is due to saturation of magnetic core which in turn due to an sudden change in the system voltage which may be caused by switching transients and out-of-phase synchronization of a generator or restoration after the clearance of fault. It decreases slowly due to the damping effect of winding resistance and takes several cycles to settle to normal current value. The value of inrush current depends on the core material, residual flux and instant of energization. Other than energization inrush current in power transformer also occurs during voltage recovery after the clearance of an external fault or after the energization of a transformer in parallel with a transformer that is already connected to power system. It contains dc offset, odd harmonics and even harmonics. Second harmonic content initially i.e. during starting is less and increases as the magnitude of inrush current decreases. Rate of decrease of unipolar inrush current is less in comparison to bipolar inrush current. The main problem associated with magnetizing inrush current is false operation of differential relay based on second harmonic restrain method in addition to damage of power transformer windings by increasing the mechanical forces like short circuit current if remain in a high value for longer time.

2.2 Mathematical derivation of inrush current

A power transformer is considered whose core is initially unmagnetized. The transformer primary winding is connected to a supply voltage v(t) and the secondary is made open.

The supply voltage is given by

$$v(t) = V_m \sin(\omega t) \tag{2.1}$$

the applied voltage is expressed as a function of flux in the core and primary current.

The applied voltage is given by

$$v(t) = Ri(t) + N \frac{d\phi(t)}{dt} \tag{2.2}$$

By neglecting the core loss and resistance equation (2.2) now becomes

$$v(t) = N \frac{d\phi(t)}{dt} \tag{2.3}$$

$$\Rightarrow \phi(t) = \frac{1}{N} \int_{-\infty}^{t} v(t)\, dt \tag{2.4}$$

$$\Rightarrow \phi(t) = \phi_{residual} - \phi_m[\cos(\omega t) - \cos(\omega t_0)] \tag{2.5}$$

$$\phi_m = \frac{V_m}{N\omega} = \frac{\sqrt{2}\,V}{N\omega} \tag{2.6}$$

$$\Rightarrow \phi(t) = -\phi_m[\cos(\omega t)] + C \tag{2.7}$$

The second term in the equation (2.7) is the integration constant and its value depends on the residual flux in the transformer core and the phase angle of the applied voltage at the instant of switching during energization. The inrush current signal during the energization of a transformer is given in Fig 2.1.
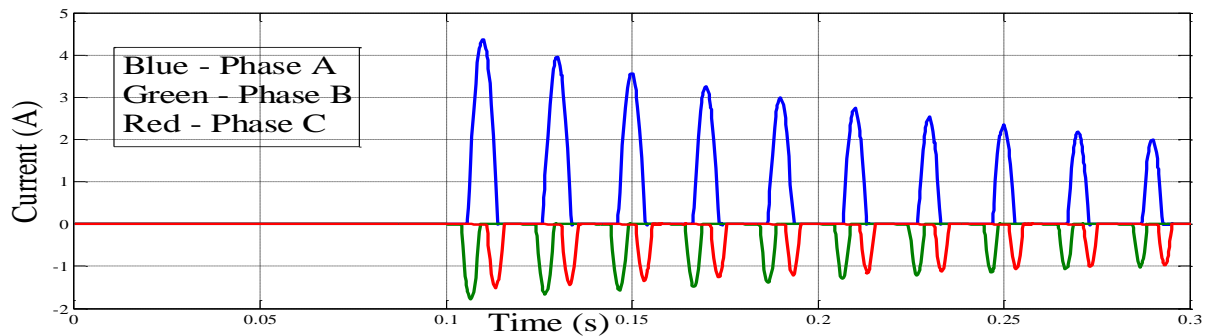
Fig. 2.1 Differential inrush current of all the three phases of a power transformer

If the transformer is energized when the voltage is at its peak then the flux is given by equation (2.8).

$$\Rightarrow \phi(t) = -\phi_m[\cos(\omega t)] \tag{2.8}$$

Transformer residual flux is neglected i.e. $\phi_{residual} = 0$

Hence it is clear from the above equation that the constant C is zero. There is no transient in flux and the time variation of flux is

$$\phi(t) = \phi_m \sin\left(\omega t - \frac{\pi}{2}\right) \qquad \text{(For } \omega t > \frac{\pi}{2}\text{)} \tag{2.9}$$
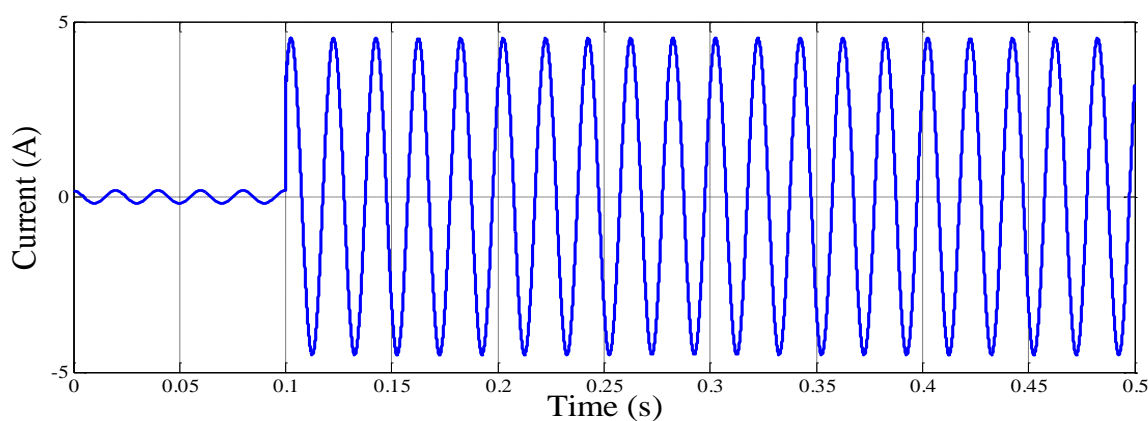
Fig. 2.2 Inrush current when the switching angle is 90 degree

If the transformer is energized when the voltage is zero then the flux is given by equation (2.9).

$$\Rightarrow \phi(t) = -\phi_m[\cos(\omega t)] + \phi_m \tag{2.9}$$

Transformer residual flux is neglected i.e. $\phi_{residual} = 0$

It is clear from the equation (2.9) that the constant C is equal to ϕ_m.

This equation shows that the flux can reach up to $2\phi_m$ at $\omega t = \pi$ which is double the peak value of the steady state flux in the transformer core under normal operating conditions. The inrush current is given in Fig 2.3 for the transformer that is energized when the voltage is at zero. It is clear that the inrush current in this case is much higher in comparison to the inrush current obtained during energization at voltage angle 90^0 given in Fig 2.2.
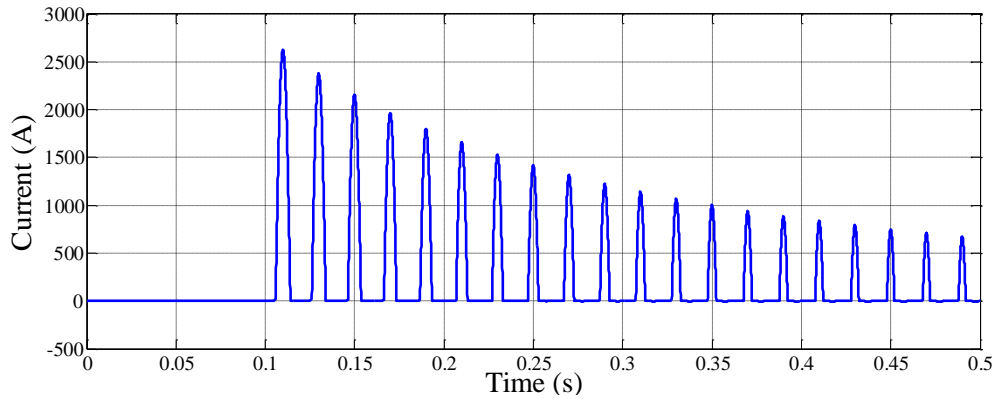
Fig. 2.3 Inrush current when the switching angle is 0^0

The analysis of inrush current predicts that excessive flux can build up in the transformer core depending on the instantaneous magnitude of the applied voltage and the residual flux at the instant of applying the voltage to the transformer.

2.3 Summary of discussion

Transformer switching phenomenon being random makes the magnetizing inrush also random. During energisation large magnitudes of currents flow into the primary winding of a transformer while no currents flow out of the secondary winding. This is similar to the conditions occurring during internal faults. Hence there arises a chance of incorrect tripping of the circuit breaker. Therefore it is necessary to distinguish between an internal fault and a magnetizing inrush current condition.

2.4 Principle of differential relay

Principle of differential protection scheme is one simple conceptual technique. The simple differential relay actually compares between primary current and secondary current of power transformer. If an unbalance between primary and secondary currents detected then the relay will actuate and inter trip both the primary and secondary circuit breaker of the transformer. In general we can say the simple differential relays operate when the vector difference of two or more similar electrical quantities at the two ends of a protection zone exceeds a predetermined level. Most simple differential relay applications are based on the current balance principle i.e. the currents at the two ends of the system are continuously compared by a suitable relay.

In practice simple differential relays suffer from drawbacks due to non-linear phenomena such as current transformer characteristics, transformer ratio change, magnetizing

10

inrush current and transformer over excitation. These cases operate the differential relay during no fault condition of transformer protection zone.

In order to overcome the problems associated with simple differential relay percentage differential relays have been developed for the protection of large power transformer. In order to avoid mal operation of the differential relay because of magnetizing inrush and transformer over excitation early practice was to delay the relays for a short time until the magnetizing inrush currents had decayed to an acceptable value. Now in practice it is provided restraint or blocking to the relays which depends on the harmonic component of the magnetizing inrush currents.

2.5   Digital relays

Modern power systems are complex networks. The complexity of these networks demands the relays used for protection to be reliable, secure, accurate and short decision making time. With the development of very large scale integrated (VLSI) chips and microprocessors the demand of modern day complex power systems can be fulfilled. A subtle shift in the paradigm takes place when we move on to the microprocessor based relay, which works on numbers representing instantaneous values of the signals. With the advent of digital relays the emphasis has shifted from hardware to software. Digital relays are programmable information processors instead of torque balancing devices. In comparison to the conventional non numerical relays that are go-no-go devices and perform only comparison the digital relays has the ability to perform real time computation.

CHAPTER- 3

ARTIFICIAL NEURAL NETWORKS

AND

WAVELET TRANSFORM

3.1 General

Neural network or artificial neural network (ANN), as the name indicates, is the interconnection of artificial neurons that tends to simulate the nervous system of a human brain. It is also defined in a literature as a neurocomputer or a connectionist system. Neurocomputing is a more generic form of artificial intelligence than expert system and fuzzy logic. In general a neural network is a massively parallel distributed processor made up of simple processing units, which has a natural propensity for storing experimental knowledge and making it available for use. It resembles the brain in two aspects

1. Knowledge required by the network from its environment through a learning process.
2. Interneuron connection strengths, known as synaptic weights, are used to store the acquired knowledge.

A biological neuron is a processing element that receives and combines signals from other neurons through input paths called dendrites. If the combined signal is strong enough, the neuron "fires", producing an output signal along the axon that connects to dendrites of many other neurons. The axon of a neuron is very long and thin and is characterized by high electrical resistance and very large capacitance. Each signal coming into a neuron along a

dendrite passes through a synaptic junction. This junction is an infinitesimal gap in the dendrite, which is filled with neurotransmitter fluid that either accelerates or retards the flow of electric charges. The fundamental actions of the neuron are chemical in nature, and this neurotransmitter fluid produces electric signals that go to the nucleus or soma of the neurons. The adjustment of the impedance or conductance of the synaptic gap leads to "memory" or "learning" process of the brain. According to this theory we lead to believe that the brain has the characteristics of "associative memory" and does not have computers like CPU and central storage memory.

A neural microcircuit refers to an assembly of synapses organized into patterns of connectivity to produce a functional operation of interest. A neural microcircuit may be likened to a silicon chip made up of an assembly of transistors.

The model of an artificial neuron that closely matches a biological neuron is given by an op-amp summer-like configuration. The artificial neuron is also called a processing element, a neurode, a node, or a cell. The input signals are normally continuous variables instead of discrete pulses that occur in a natural neuron. Each of the input signals flows through a gain or weight, called synaptic weight or connection strength whose function is analogous to that of the synaptic junction in a natural neuron. The weights can be positive (excitory) or negative (inhibitory) corresponding to acceleration or inhibition respectively. The summing node accumulates all the input-weighted signals and then passes to the output through the transfer function, which is usually nonlinear.

3.2 Training of ANN

The process of modifying the weights in the connections with the objective of achieving the expected output is called training a network. The internal process carried out during training is called learning.

Training is grouped into three categories.

1. Supervise Training
2. Unsupervised Training
3. Reinforced Training or Neurodynamic Programming
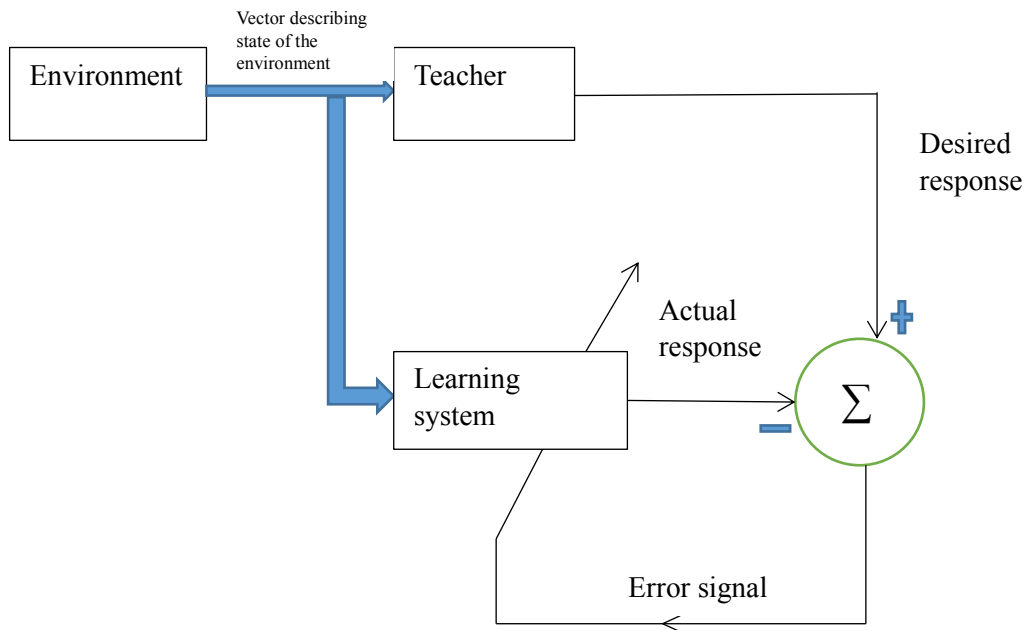
Fig. 3.1 Block diagram of supervised learning

3.3 Activation function

The activation function can be any function that is monotonically increasing and differentiable. The sigmoid function is the most popular activation function because it resembles the behaviour of many biological neurons.

Some commonly used activation functions are

1. Identity function
2. Threshold function or Heaviside function
3. Piecewise-Linear function
4. Sigmoid function

3.4 Multilayer feedforward ANN

The basic multilayer feedforward network contains three layers namely input, output and hidden. This type of neural network has one input layer, one output layer and any number of hidden layers in between the former two layers. Each network layer contains processing units called nodes or neurons. Each node in a network layer will send its output to all the nodes of the next layer. In the input layer the nodes receive signals from the

outside world. The input layer of the neural network serves as an interface that takes information from the outside world and transmits that to the internal processing units of the network, analogous to a human's interface parts such as our eyes' retina and our fingers' sensing cells. Similarly the output layer of the neural network serves as an interface that sends information from the neural network's internal processing units to the external world. The nodes in the hidden layer are the neural network's processing units. The number of hidden layers and the numbers of neurons in each hidden layer depend on the network design considerations. The input layer transmits the signal to the hidden layer, and the hidden layer in turn transmits the signals to the output layer. There is no self, lateral or feedback conversion of neurons.
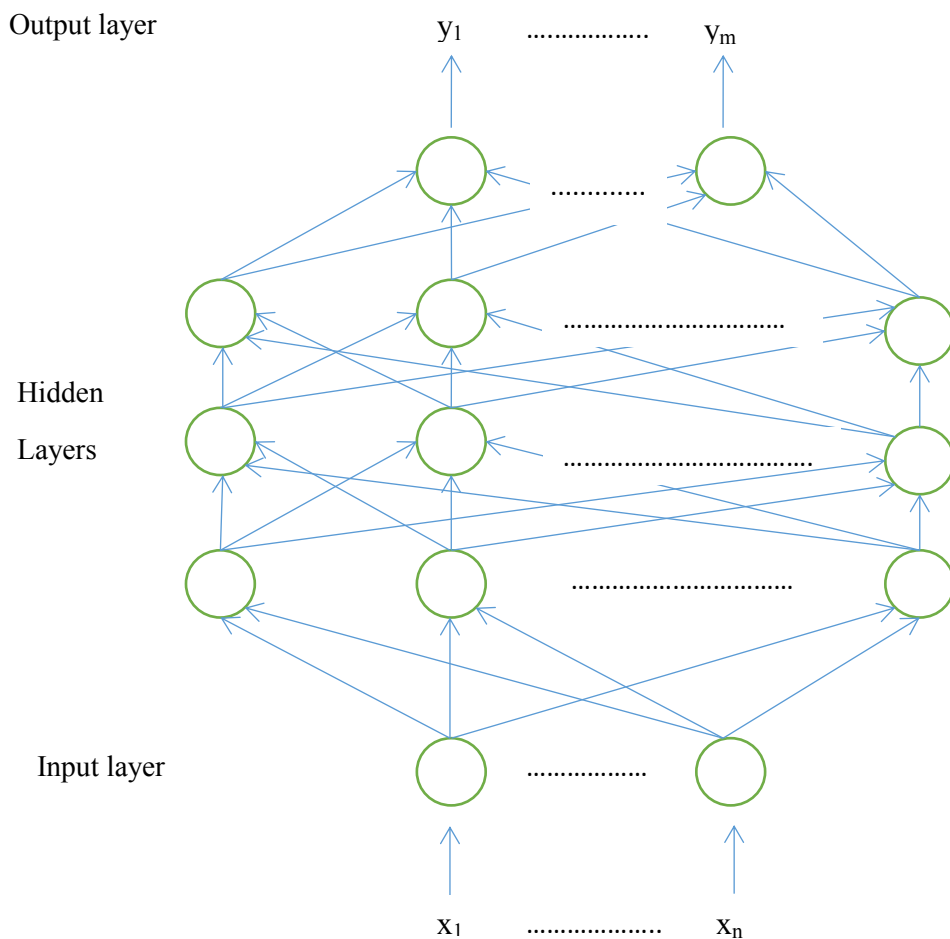
Fig. 3.2 Basic structure of a multilayer feedforward ANN

3.5 Model of a neuron
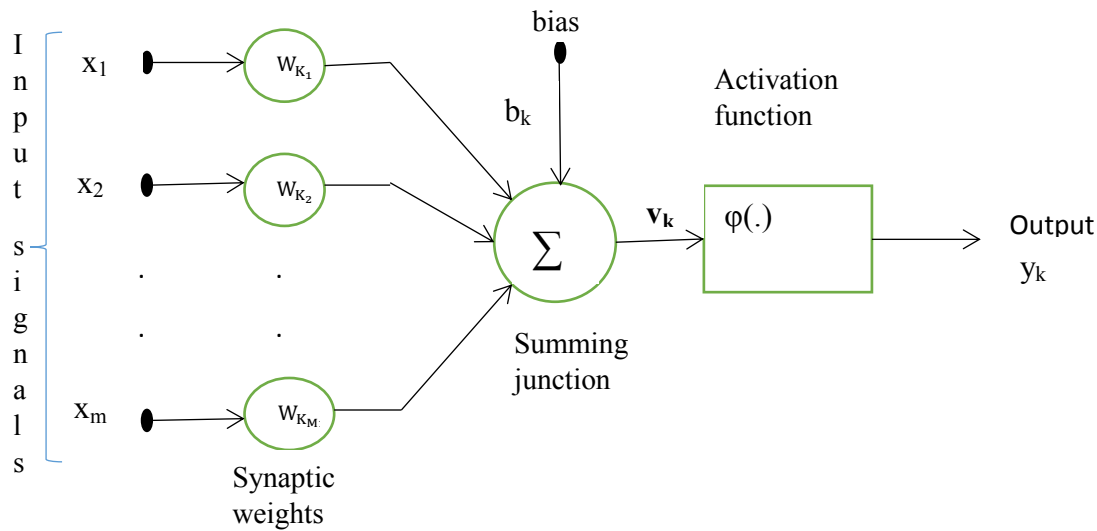
Fig. 3.3 Model of a neuron

A signal x_j at the output of synapse j is connected to neuron k is multiplied by the synaptic weight w_{k_j}. The first subscript of the synaptic weight refers to the neuron and the second synaptic weight refers to the input end of the synapse to which the weight refers. The neuron model also includes an externally applied bias, denoted by b_k. The bias b_k has the effect of increasing or lowering the net input of the activation function, depending on whether it is positive or negative respectively.

3.6 Back propagation training algorithm

Back Propagation (BP) learning algorithm is used to train the multi-layer feed-forward neural network. Signals are received at the input layer, pass through the hidden layer, and reach to the output layer, and then fed to the input layer again for learning. The learning process primarily involves determination of connection weights and patterns of connections. The BP neural network approximates the non-linear relationship between the input and the output by adjusting the weight values internally instead of giving the function expression explicitly. Further, the BP neural network can be generalized for the input that is not included in the training patterns. The BP algorithm looks for minimum of error function in weight space using the method of gradient descent. The combination of weights that minimizes the error function is considered to be a solution to the learning problem.

The training algorithm of back propagation involves four stages, i.e.

1. Initialization of weights
2. Feed forward
3. Back propagation of errors
4. Updation of the weights and biases

During first stage, i.e. the initialization of the weights, some random variables are assigned. During feed forward stage each input unit (X_i) receives an input signal and transmits this signal to each of the hidden units z_1....z_p. Each hidden unit then calculates the activation function and sends its signal z_j to each of the output unit. The output unit calculates the activation function to form the response of the network for the given input pattern. During back propagation of errors, each output unit compares its compound activation function y_k with its target value t_k to determine the associated error for that pattern with that unit. Based on the error, the factor δ_k (k=1,...., m) is computed and is used to distribute the error at output unit y_k back to all units in the previous layer. Similarly the factor δ_j (j= 1,...., p) is computed for each hidden unit z_j. During final stage, the weight and biases are updated using the δ factor and the activation. The step by step algorithm is given below [2].

Initialization of weights

Step 1: Weights are initialized to small random values between 0 to1.

Step 2: While stopping condition is false, steps 3-10 are repeated.

Step 3: For each training pair steps 4-9 are performed.

Feed forward

Step 4: Each input node receives the input signal x_i and transmits that to all nodes in the layer above, i.e. to the hidden units.

Step 5: Each hidden unit (z_j, j=1,.....,p) sums the weighted input signals.

$$z_{in_j} = V_{o_j} + \sum_{i=1}^{n}(x_i \cdot V_{i_j}) \tag{3.1}$$

Applying the activation function

$$Z_j = f\left(z_{in_j}\right) \tag{3.2}$$

And this signal is sent to all the units in the layer above, i.e. to output units.

Step 6: Each output unit (y_k, k=1,….., m) sums its weighted input signals.

$$y_{in_k} = W_{o_k} + \sum_{j=1}^{p}(z_j W_{jk}) \tag{3.3}$$

And activation function is applied to calculate the output signals.

$$Y_k = f\left(y_{in_k}\right) \tag{3.4}$$

Back Propagation of errors

Step 7: Each output unit (y_k, k=1,….., m) receives a target pattern corresponding to an input pattern. Error information term is calculated as follows

$$\Delta_k = (t_k - y_k)f^1(y_{in_k}) \tag{3.5}$$

Where $f^1\left(y_{in_k}\right) = f(y_{in_k})(1 - f(y_{in_k}))$ \hfill (3.6)

Step 8: Each hidden unit (z_j, j=1,…..,p) sums its delta inputs from units in the layer above.

$$\delta_{in_j} = \sum_{k=1}^{m}(\delta_j W_{jk}) \tag{3.7}$$

The error term is calculated as

$$\delta_j = \delta_{in_j}f^1\left(z_{in_j}\right) \tag{3.8}$$

Where $f^1\left(z_{in_j}\right) = f(z_{in_j})(1 - f(z_{in_j}))$ \hfill (3.9)

Updation of weight and biases

Step 9: Each output unit (y_k, k=1,….., m) updates its bias and weights (j=0,……..,p)

The weight correction term is given by

$$\Delta W_{jk} = n\delta_k z_j \tag{3.10}$$

And the bias correction term is given by

$$\Delta W_{o_k} = n\delta_k \tag{3.11}$$

Therefore

$$W_{jk}(new) = W_{jk}(old) + \Delta W_{jk} + m\left[W_{jk}(old) - W_{jk}(old - 1)\right] \tag{3.12}$$

And

$$W_{o_k}(\text{new}) = W_{o_k}(\text{old}) + \Delta W_{o_k} \tag{3.13}$$

Each hidden unit (z_j, j=1,…..,p) updates its bias and weight(i=0,….,n)

The weight correction term is

$$\Delta V_{i_j} = n\delta_j x_i \tag{3.14}$$

And the bias correction term is

$$\Delta V_{o_j} = n\delta_j \tag{3.15}$$

Therefore

$$V_{i_j}(\text{new}) = V_{i_j}(\text{old}) + \Delta V_{i_j} + m\left[V_{i_j}(\text{old}) - V_{i_j}(\text{old} - 1)\right] \tag{3.16}$$

And

$$V_{o_j}(\text{new}) = V_o(\text{old}) + \Delta V_{o_j} \tag{3.17}$$

Step 10: The stopping condition is checked (minimization of the errors).

3.7 Summary of discussion of ANN

ANN can be implemented for fault and inrush current classification without the need of exact mathematical relationship between input and output. ANN has been widely used because of their multi input parallel processing capability. The increase in number of nodes doesn't affect the computation time of the network as it perform parallel processing. Increasing the number of input nodes increase the robustness of the ANN.

3.8 Fundamental of WT

The Fourier transform is a useful tool to analyse the frequency components of the signal. But Fourier transform is silent about the instant at which a particular frequency appears. Short-time Fourier transform (STFT) uses a sliding window to find spectrogram, which gives the information of both time and frequency. But in case of STFT the length of window is fixed for all frequency. The ability of wavelet transform (WT) to focus on short time intervals for high-frequency components and long intervals for low-frequency components improves the analysis of signals with localised impulses and oscillations. For this reason wavelet decomposition is ideal for studying transient signals and obtaining a much better current characterisation and a more reliable discrimination.

In wavelet analysis the signal to be analysed is multiplied with a wavelet function called mother wavelet just as it is multiplied with a window function in STFT. In WT, the width of the wavelet function changes with each spectral component. During the analysis less time is given for higher frequencies and more time is given for low frequencies. For high frequency, the WT gives good time resolution for low frequencies, the WT gives good frequency resolution.
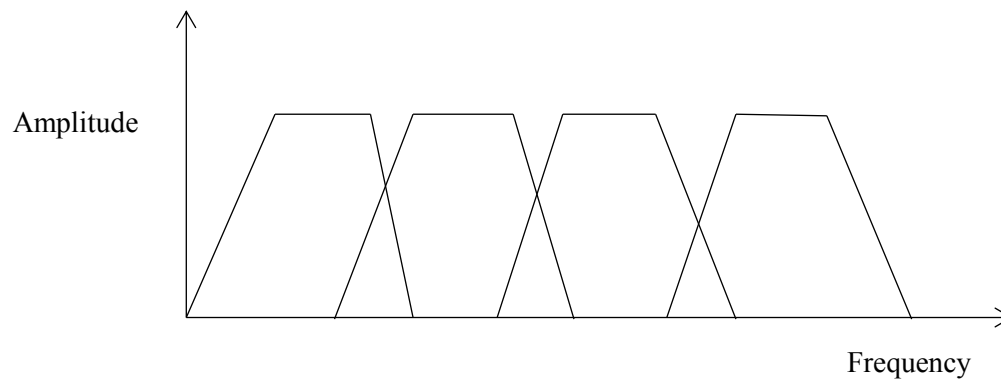
(a) STFT
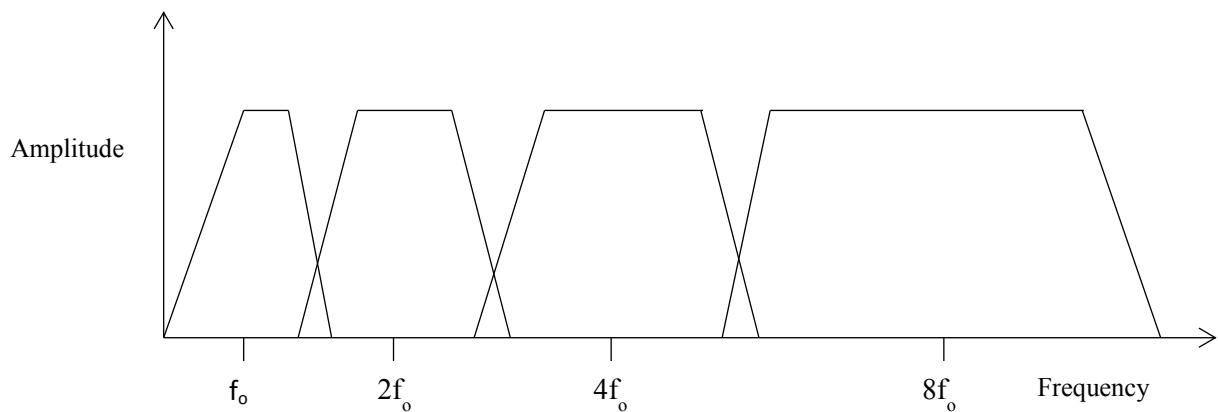
(b) DWT

Fig. 3.4 Comparison of (a) the STFT uniform frequency coverage to
(b) The logarithmic coverage of the DWT.

3.9 Need of WT

Current signals during the occurrence of fault and during inrush condition of power transformer are associated with fast electromagnetic transients. These signals are typically non-periodic and contain both high-frequency oscillations and localised impulses superimposed on the power frequency and its harmonics. This characteristic creates a

problem for traditional Fourier analysis because it assumes a periodic signal. As power system disturbances are subject to transient and non-periodic components, the DFT alone can be an inadequate technique for signal analysis. Thus WT is a powerful tool in the power system transient phenomena analysis. It has the ability to extract information from the transient signals simultaneously in both time and frequency domains and has replaced the Fourier analysis in many applications. A WT expands a signal not in terms of a trigonometric polynomial but by wavelets, generated using the translation (shift in time) and dilation (compression in time) of a fixed wavelet function called the mother wavelet. The wavelet function is localised in time and frequency yielding wavelet coefficients at different scales (levels). This gives the wavelet transform much greater compact support for the analysis of signals with localised transient components.

3.10 Discrete wavelet transform

Discrete Wavelet Transform (DWT) gives faster analysis in comparison to continuous wavelet transform as it is based on sub-band coding. In DWT, digital filtering techniques enable a time-scale representation of the digital signal. The signal analysis process is nothing but the travel of signal through filters with different cut off frequencies at different scales.

3.11 DWT and filter banks

The signal resolution is determined by the filtering operations and is a measure of the amount of detail information in the signal whereas the scale is determined by up sampling and down sampling operations. Down sampling a signal corresponds to reducing the sampling and up sampling a signal corresponds to increasing the sampling rate.

The DWT is computed by successive low pass and high pass filtering of the discrete time-domain signal in one algorithm called the Mallat algorithm or Mallat-tree decomposition given in Fig 3.5. Initially an original signal is divided into two halves of the frequency bandwidth and given to high pass (H_0) and low pass (G_0) filter. Then the output of the low pass filter is again half the frequency bandwidth and fed to second stage. This procedure is repeated until the filter length becomes equal to length of the signal.

Detail coefficients are the outputs of high pass filter and the approximate information are from the low pass filter. Frequency band of each detail is directly related to the sampling rate of original signal. At each detail level the frequency become halved of the previous stage as per Nyquist's theorem.
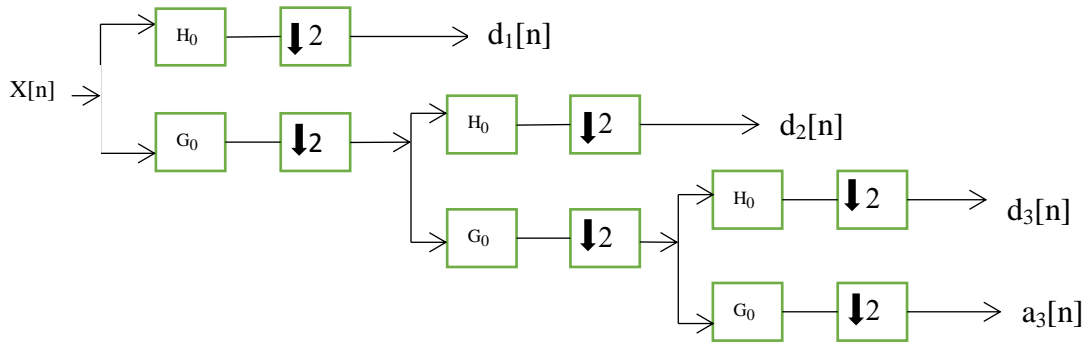
Fig. 3.5 Implementation of DWT

3.12 Comparison of DWT with other transforms
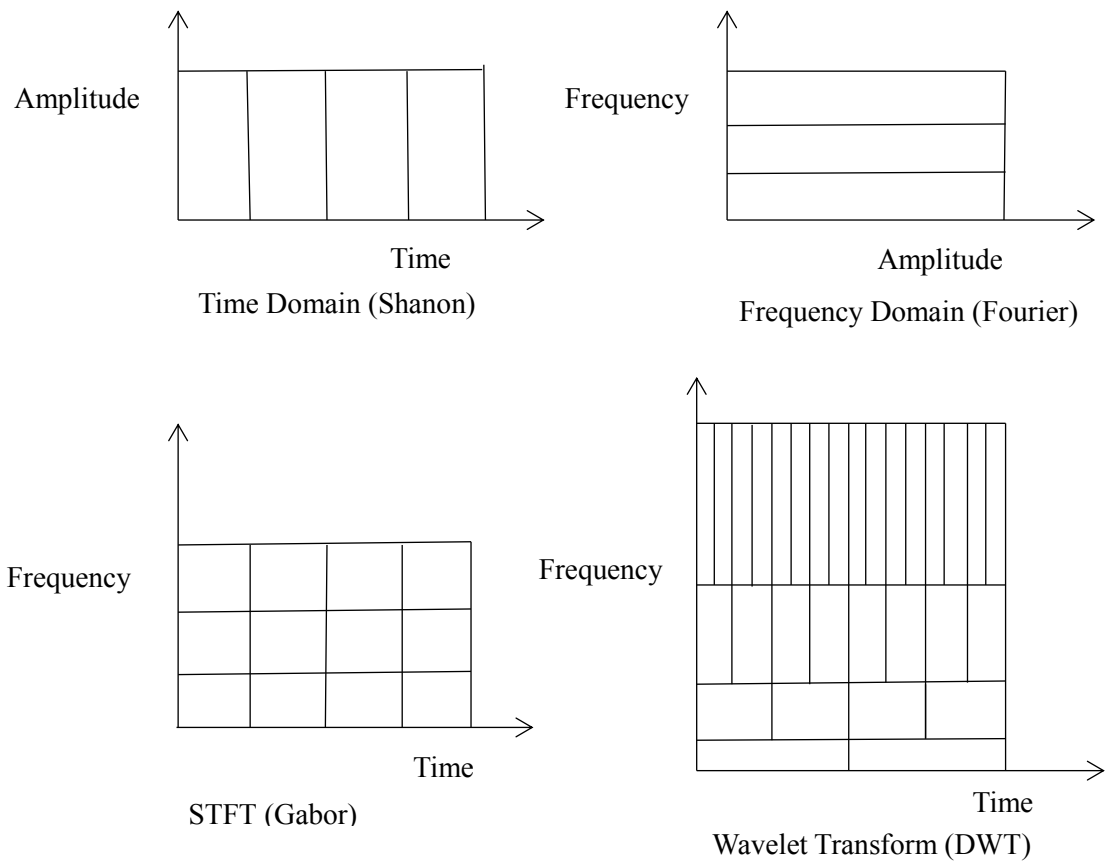
Fig. 3.6 Comparison of DWT with other transforms

3.13 Implementation of WT

Out of a large list of mother wavelets available, the choice of a particular mother wavelet plays an important role in detecting and classifying different types of fault and inrush transients of power transformer. Since the transformer transient study deals with analysing short duration, fast decaying current signals therefore Daubichies's mother wavelet of level 6 (D6) is used in this thesis.

The wavelet analysis of various transient current signals obtained from SIMULINK result in different conditions like: normal, inrush, internal and external fault and over excitation are carried out. The starting sampling frequency is 20 kHz. All the current signals considered in wavelet analysis are taken from a star-star and a delta-star transformer connected in a power system (system specification given in appendix-1).

CHAPTER- 4

DFT ANALYSIS

AND

SIMULATED TRANSIENT SIGNALS

4.1 General method

The DFT of the simulated transient current signals obtained for various conditions of a power transformer (star-star) connected to a power system are obtained using fast Fourier transform (FFT) algorithm. The objective of this analysis is to show the harmonic content during the transient period. The conventional differential protection scheme that are based upon second harmonic restrain assume that only inrush current is reach in second harmonic component. This is only valid if our relay operation time will be more than one cycle or 20 m sec. But if we are interested to detect the fault in a period less than one cycle, which is the major concern of current and future smart power transmission system then the harmonic content of all the transient signals differs from the traditional values. My findings predict that if very less transient time is considered i.e. if the window for FFT analysis is taken to be 20 m second i.e. one cycle taking the fundamental frequency of power transmission as 50 Hz, starting just before the occurrence of transient event then the second harmonic content of the various current signals during fault are either nearer to that of inrush current or higher than that. As I considered the FFT window of length 20 m sec starting just before the event, therefore it accounts any transient event that lasts for less than a cycle after its occurrence.

4.2 Normal operating condition
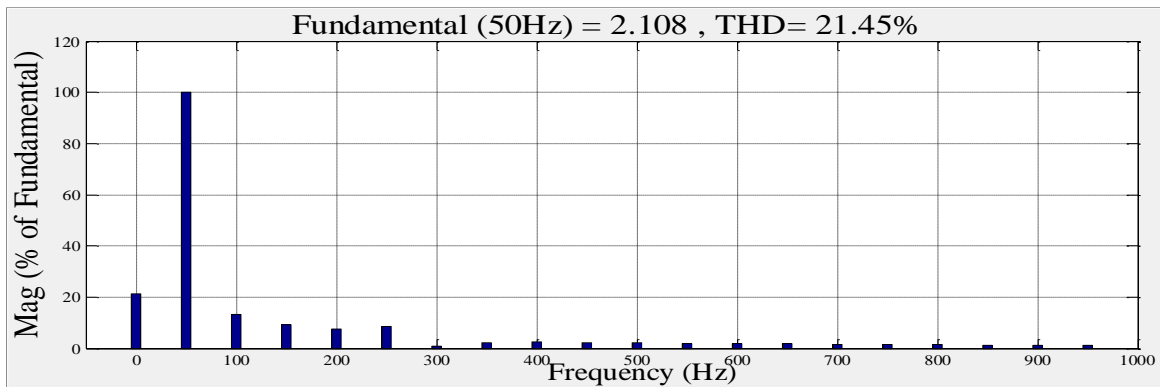
Fig. 4.1 A phase differential current

The above FFT plots shows that during normal case the percentage of second harmonic current is very less in comparison to fundamental and in this case there is no problem with the conventional relay. Those relays will remain dormant in this case as the ratio of inrush to fundamental is negligible and that matches with their algorithm. The relays can only issue a trip command to the circuit breaker if the ratio exceeds a predefined limit which is formed by taking the inrush current case as the base or reference.

4.3 Inrush condition
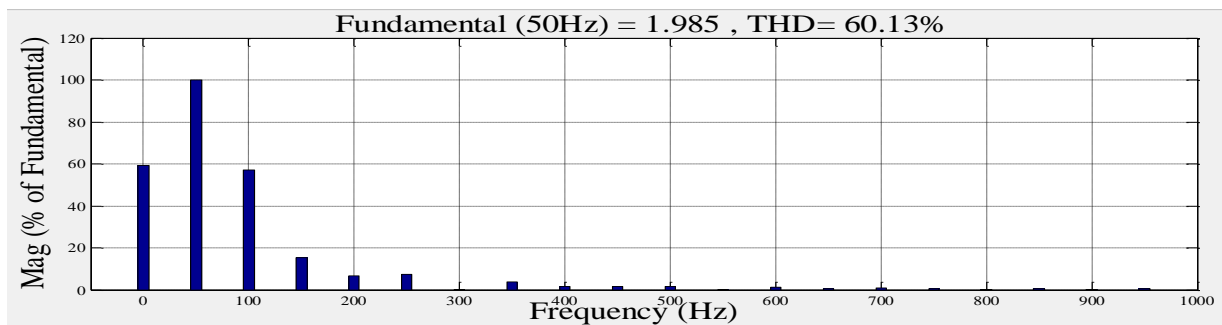
Fig. 4.2 A phase differential current
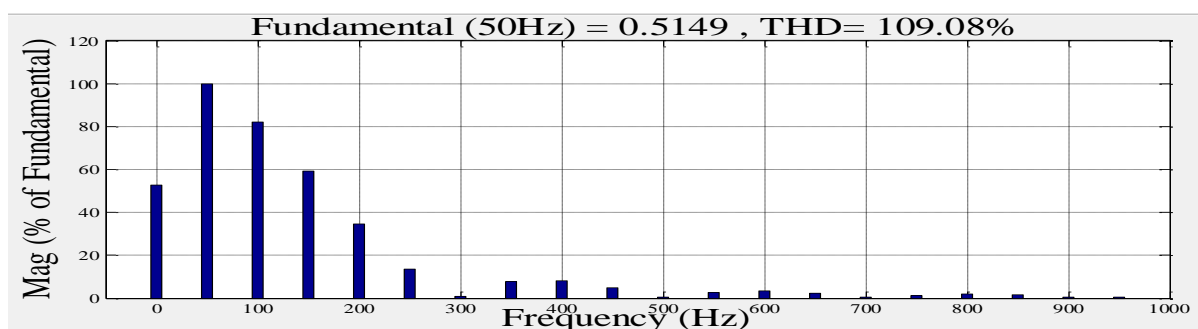
Fig. 4.3 B phase differential current

25
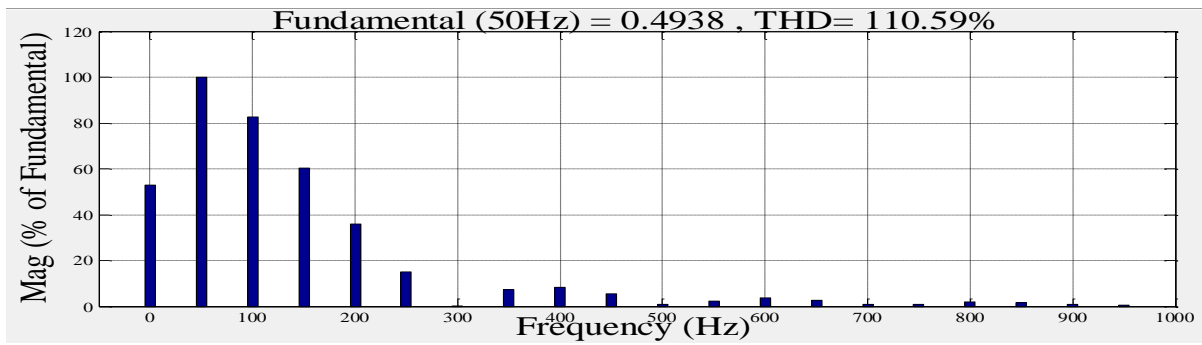
Fig. 4.4 C phase differential current

During the FFT analysis of inrush case transient currents for one cycle it is seen that the percentage of second harmonic content is different for the three phases. The percentage second harmonic content is of significant amount. The conventional relay will work in this case but the detection and algorithm will fail if the relay operating time will be taken less than a cycle and also if the transient phenomena lasts for less than a cycle. The conventional algorithm starts the FFT window from the starting of the event resulting less percentage of second harmonic content. But the analysis of the transient current signal for less than a cycle also predicts a large mismatch among the three phase contents as far as second harmonic factor is considered.

4.4 L-L-L-G fault case
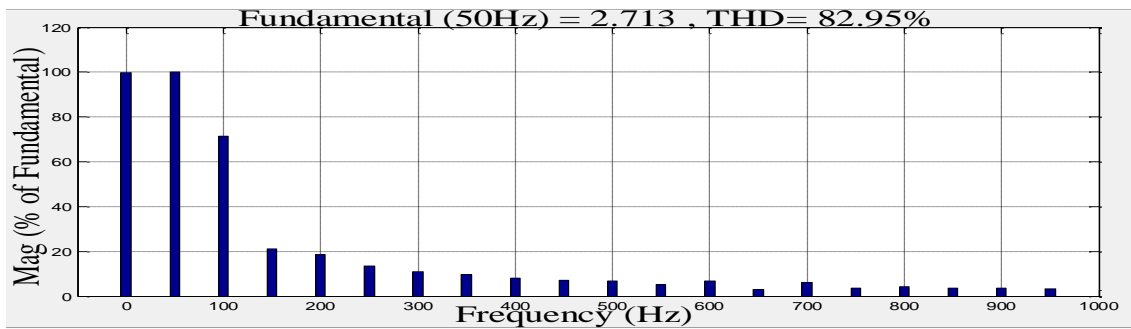
Fig. 4.5 A phase differential current
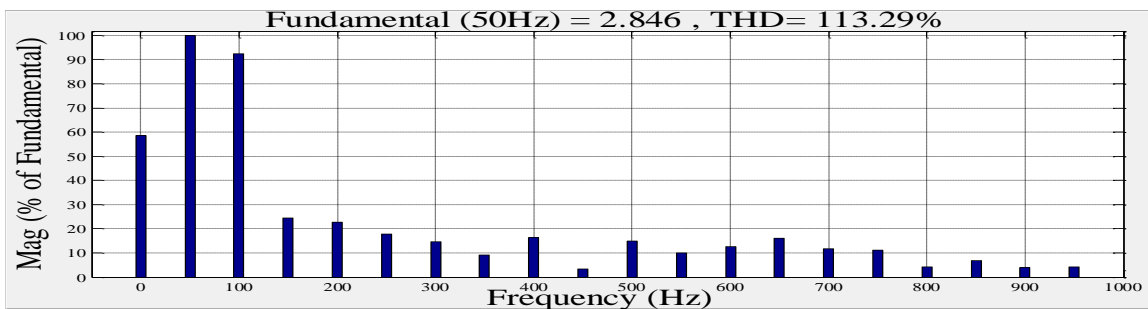
Fig. 4.6 B phase differential current

26
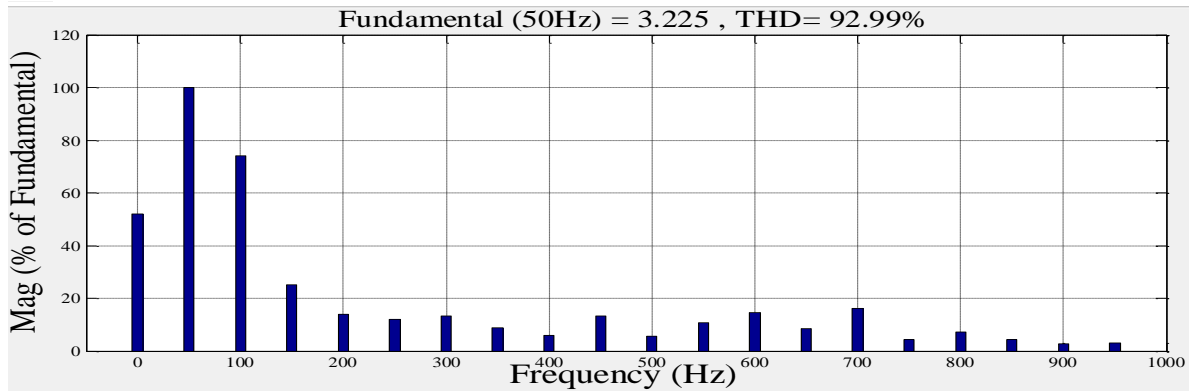
Fig. 4.7 C phase differential current

The FFT analysis of different internal faults (fault inside the protection zone of transformer) like single line to ground fault (L-G), double line to ground fault (L-L-G) and three phase line to ground fault (L-L-L-G) situations are analysed. It is clear that the percentage of second harmonic component in the transient current of power transformer is more or less equal to that of inrush current for phase A during L-G fault. And the percentage of second harmonic component is negligible for phase B and phase C currents for L-G fault case (less than normal case). For L-L-G fault the percentage of second harmonic component is far higher than the inrush case for phase A and phase B but negligible for phase C. In case of L-L-L-G fault the percentage of second harmonic component is higher than that of inrush case for phase B and almost equal to that of inrush case for phase A and phase B differential transient currents. Only the L-L-L-G fault case analysis is shown in Fig 4.5 to 4.7. Analysis results of other cases are given in Table 4.1.

4.5 L-L-L fault case
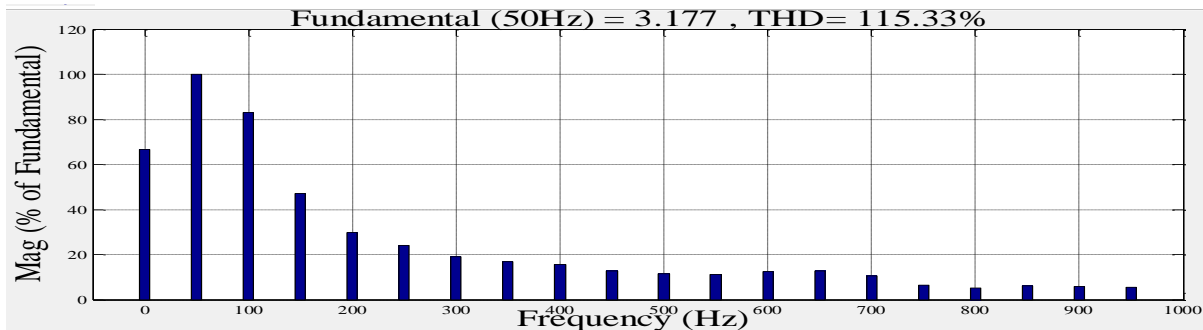
Fig. 4.8 A phase differential current

27

Two cases of internal faults like line to line fault (L-L) and three phase short circuit (L-L-L fault) are also analysed using FFT. It is observed that the percentage of second harmonic current is equal to that of inrush case for phase A and more for phase B during L-L fault. During L-L fault the phase C current has negligible amount of second harmonic component like normal operating condition.

For three phase short circuit situation the percentage of second harmonic component is higher than that of inrush case for all the three phases and are almost equal. Only the analysis of phase A current in case of L-L-L fault is given in Fig 4.8. Analysis of all other phases during line to line fault and three phase short circuit are given in Table 4.1.

4.6 External fault and over excitation case.

The FFT analysis of transient differential current during the external (fault occurring outside the protection zone of transformer) L-L-L-G fault gives the result that the percentage of second harmonic component is less in all the three phases in comparison to inrush condition. The analysis of all the three phase currents during external fault and over excitation case is given in table 4.1.

The relay based on second harmonic restrain will show correct result for external case. But my objective deals with correct performance of differential relay during internal fault and inrush case. So this case is not so much important as the objective of this research is concerned. The FFT analysis is not sufficient for the relay based on DFT to discriminate external fault from normal and internal fault situation as the ratio of percentage of second harmonic component to fundamental is also less than that of inrush for normal case.

During over excitation (sudden change in load more than rated capacity) leads to flow of large current in the transformer winding. But the differential relay based on second harmonic restrain principle or DFT as a background will not be able to detect that because the percentage of second harmonic component is almost equal to that of normal operating condition for all the three phases in case of over excitation.

The percentage of second harmonic for all the possible simulated cases in all the three phases are given in a tabular manner in Table 4.1 for star-star transformer and in Table 4.2 for delta-star transformer. The primary of the delta-star transformer is connected in D11 and the secondary is connected in Y fashion. In case of star-star both the windings are connected in Yg manner.

Table 4.1 Percentage of second harmonic content in the differential current in various conditions in case of star-star transformer

Type of condition	Phase A	Phase B	Phase C
Normal	15.23	4.76	17.86
Inrush	**57.69**	**82.47**	**83.47**
L-G fault	**71.16**	0.76	1.12
L-L-G fault	**80.66**	**93.39**	0.86
L-L-L-G fault	**72.14**	**92.58**	**76.23**
L-L fault	**61.31**	**78.46**	0.64
L-L-L fault	**82.16**	**91.36**	**82.75**
External fault	25.14	24.26	42.14
Over excitation	17.16	12.26	18.14

The red marked values denotes the percentage of second harmonic component in the differential current of magnetizing inrush current and the values marked in blue indicates the percentage of second harmonic component in the differential current of various faulty situations associated with the power transformer secondary terminal.

Table 4.2 Percentage of second harmonic content in the differential current in various conditions in case of delta-star transformer

Type of condition	Phase A	Phase B	Phase C
Normal	15.9	13.13	3.7
Inrush	**35.77**	**64.51**	**64.53**
L-G fault	**52.78**	15.53	0.21
L-L-G fault	**49.15**	**55.09**	19.41
L-L-L-G fault	**46.24**	**58.08**	**73.51**
L-L fault	**42.23**	**72.54**	20.37
L-L-L fault	**48.64**	**65.76**	**84.73**
External fault	**42.68**	26.77	25.83
Over excitation	15.7	14.64	10.81

4.7 Summary of discussion

The percentage of second harmonic component is not same for the three phases in a particular case. As conventional relays are not provided with artificial intelligence (AI) therefore they are not efficient in fuzzy situations like how much less or how much more. Secondly due to different methods adopted to mitigate the inrush current in power transformer itself decrease the second harmonic component in the magnetizing inrush

currents in modern day power system by the use of advanced core materials. Thirdly as the frequency content of the transient current signals is different in comparison to steady portion so the transient current is aperiodic and non-stationary during transient period. Hence the traditional DFT based algorithm is not a strong protective measure for smart power system if the interest is efficient performance of the protective relay within a cycle i.e. 20 m sec. This opens window for different advanced signal processing techniques and AI based classifier to meet the requisite demand.

WT being capable of extracting information in both time and frequency domain assuming the signal to be finite and not infinite duration as in case of DFT suits better for non-stationary and aperiodic signals like transient fault and inrush current of power transformer and has the ability to replace the traditional DFT based signal processing technique as a modern signal processing method. Similarly the ANN is a suitable classifier after proper training. Hence this research deals with WT and ANN for the discrimination of various transient situations in power transformer.

4.8 Simulated transient current signals

The power system model with both star-star and delta-star transformer are simulated in MATLAB/SIMULINK environment. The SIMULINK models are given in appendix 2. The specification of the different system parameters are given in appendix 1.All the analysis are performed in discrete domain with sampling frequency of 20 kHz.

For normal operating condition the switching circuit connecting the three phase source that acts as the alternator is switched on at 0.1 sec for all the readings of normal case. For different readings the voltage angle of the source voltage are varied. The load is fixed for all situations except over excitation case and is taken as 450 MW and 530 MVAR. Transformer primary and secondary terminals are connected in star with grounded terminal. The source is star with ground terminal. The three phase current signals coming from the differential relay during normal operating condition is given in Fig 4.9.
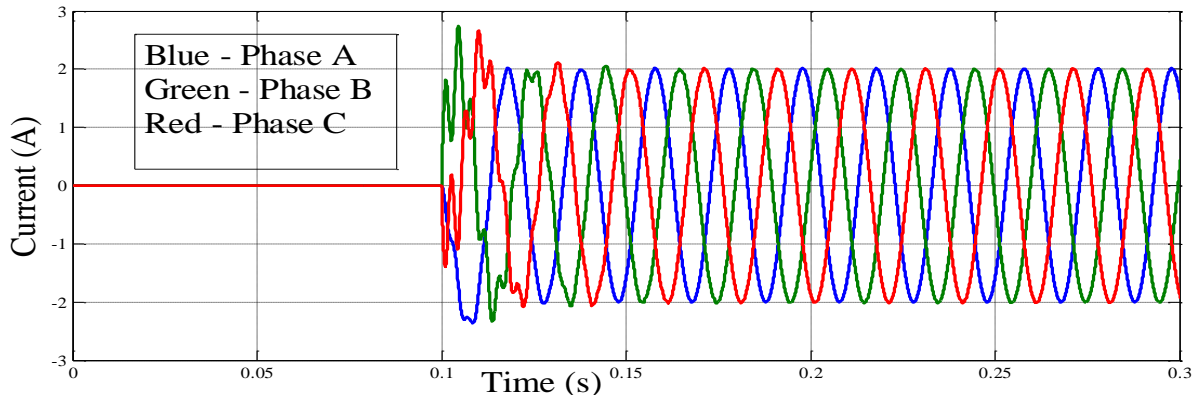
Fig. 4.9 Normal operating condition

During inrush case the transformer secondary side is kept open. The various readings are simulated by varying the switching at different angles of the source voltage. It is found that the inrush current is least if the phase is switched at 0^0 and is highest if the switching takes place at 90^0. The switching circuit connecting the source to power transformer at 0.1 sec. The three phase current signals coming from the differential relay during inrush condition is given in Fig 2.1

During the simulation of L-G fault the switching circuit connecting the source and the transformer is activated at 0.05 sec. and when the source voltage is at 0^0. The switching conditions are kept constant for various readings of the L-G fault simulation. The fault transient occurs in between 0.1 to 0.12 sec i.e. for 1 cycle. The fault resistance is varied for different readings in this situation. Other conditions are same that of normal operating condition. The L-G fault occurs in between phase A and ground on the secondary side of transformer. The fault occurs inside the protection zone of transformer. In similar situations the L-L-G and L-L-L-G cases are also simulated and transient current signals are obtained and are used in wavelet analysis. The three phase current signals coming from the differential relay during L-L-L-G fault is given in Fig 4.10.

Fig. 4.10 L-L-L-G fault

31
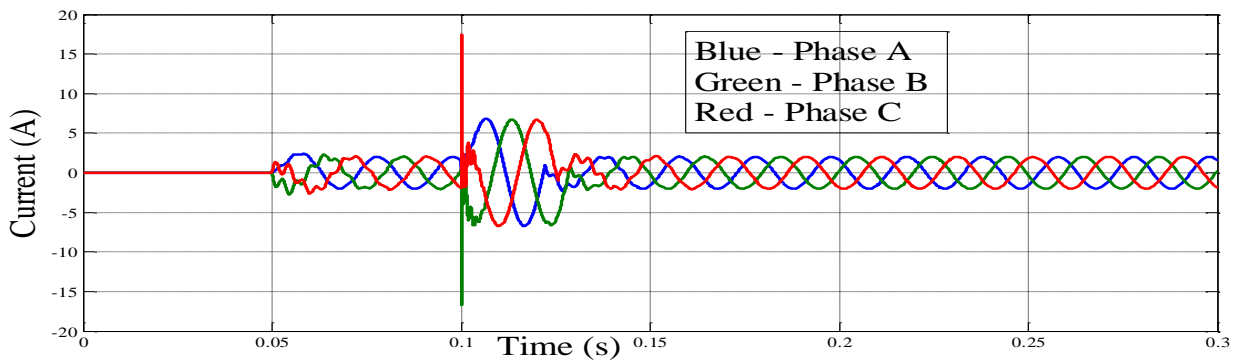
For L-L fault and three phase short circuit case all the conditions are same as that of L-G fault. The L-L fault occurs between phase A and phase B and in case of L-L-L fault all the three phases A, B and C are shorted. The three phase current signals coming from the differential relay during L-L-L fault is given in Fig 4.11.
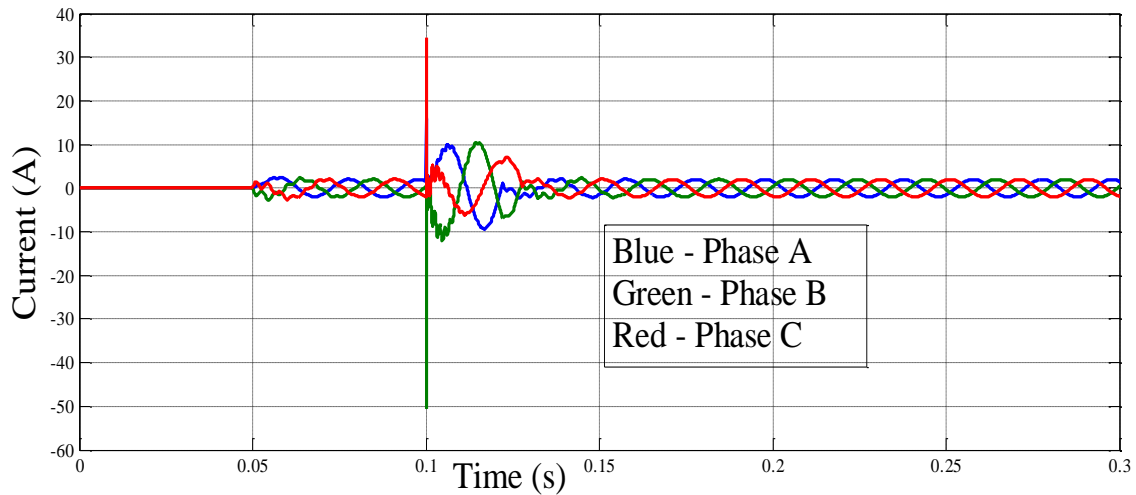
Fig. 4.11 L-L-L fault

For external fault case all the conditions are same as that of L-G fault. The external L-L-L-G fault occurs outside the protection zone of transformer among phase A, phase B, phase C and ground on the secondary side of transformer. The three phase current signals coming from the differential relay during external fault is given in Fig 4.12.
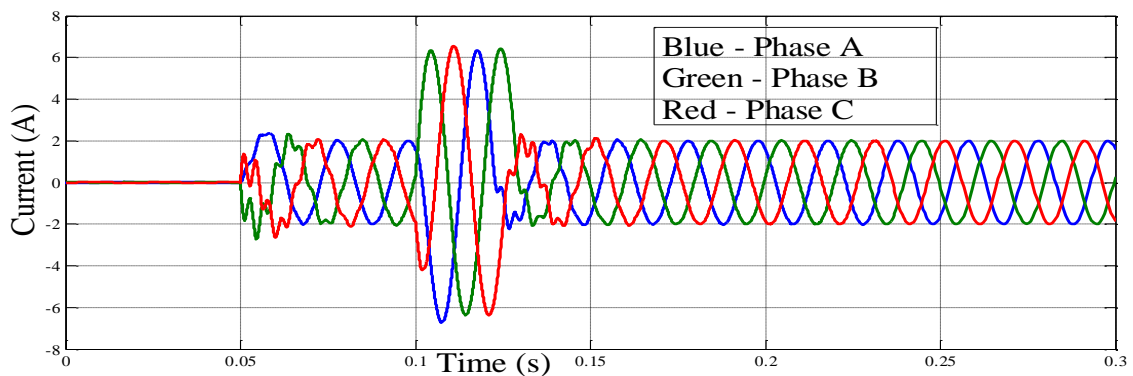
Fig. 4.12 External fault

In over excitation case instead of fault, at the same time an additional load is connected to the existing system. The switching circuit that connects the additional load is triggered at 0.1 sec. The transient duration is from 0.1 to 0.12 sec. The additional load is of 450 MW and 530

MVAR. Other conditions are same as that of L-G fault. The three phase current signals coming from the differential relay during over excitation is given in Fig 4.13.
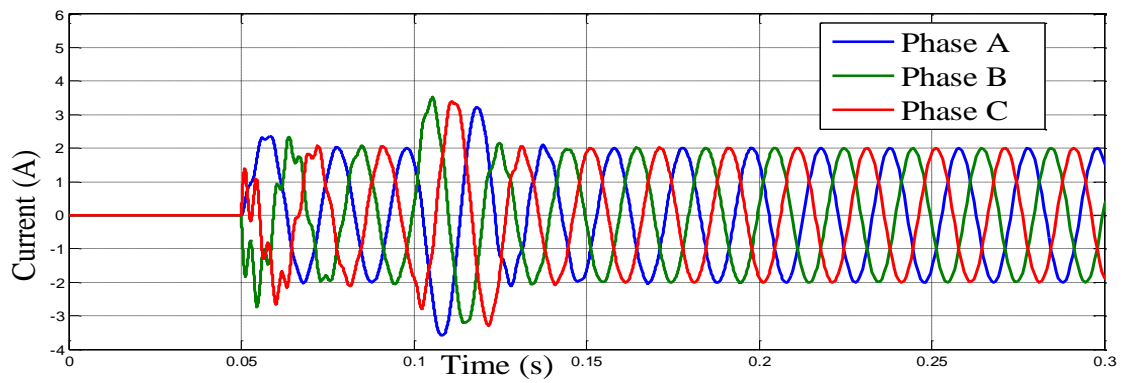

Fig. 4.13 Over excitation case

CHAPTER- 5

WAVELET ANALYSIS OF THE TRANSIENT CURRENT SIGNALS

5.1 General method

Since the transient current signals during fault, inrush and over excitation conditions are fast decaying and oscillating type of high frequency signals therefore Daubichies's wavelet of level 6 (db6) best suits for the analysis purpose. The sampling frequency is 20 kHz i.e. the original signal is sampled at 20 kHz. The highest frequency that the signal could content will be 10 kHz as per Nyquist's theorem. This frequency is observed at the output of high frequency filter which gives the first detail. Thus the band frequencies between 10 kHz to 5 kHz are captured in detail 1. Similarly the band frequencies between 5 kHz to 2.5 kHz are captured in detail 2 and so on. The wavelet analysis using db6 as the mother wavelet is performed up to detail 5 level for the differential current signals of all the cases to extract the detail coefficients. The analysis is carried out for 20 msec.

5.2 Wavelet analysis in normal case

Wavelet analysis for normal operating case at the instant when switching takes place at 0^0 angle of the source voltage is shown in Fig 5.1 and 5.2. The Fig 5.1(a) represents the original signal. In this chapter only phase A differential current is selected for the analysis. Analyses of other phases are not represented graphically. The analysis of all the three phases is performed and the data obtained from the detail coefficients in different levels are used for training of ANN. As the detail level increases the frequency of the signal content in that decreases and the time for which that is analysed increases. The frequency decrease by a factor of two and the time increase by a factor of two. The Fig 5.1 (b)-(c) and Fig 5.2 (a)-(c) represent the decomposed detail coefficient signals in different levels
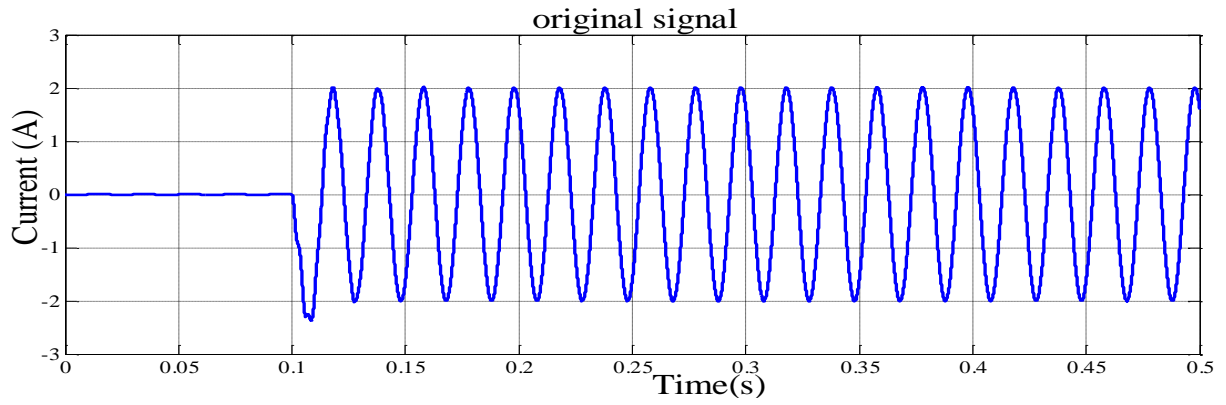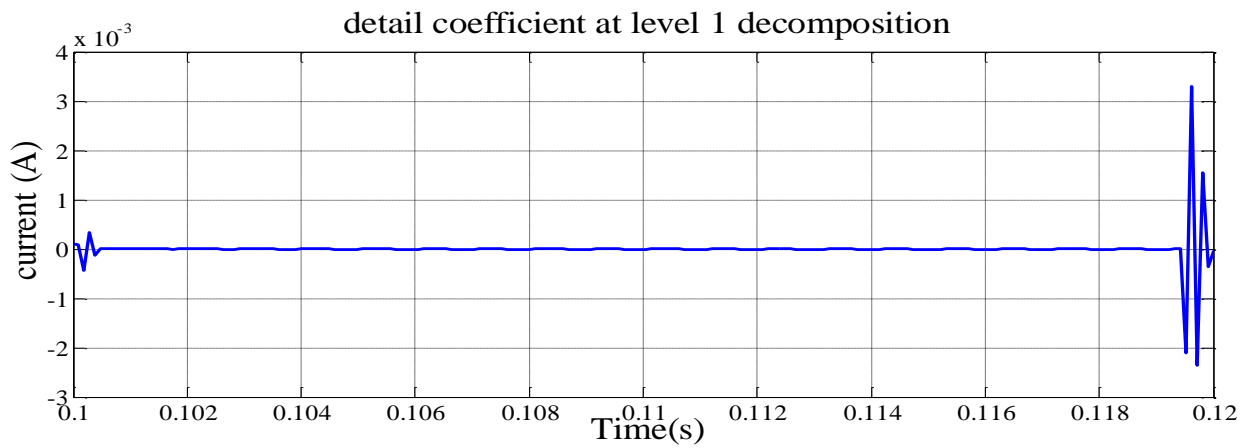
Fig. 5.1 Wavelet analysis of phase A differential current for normal case.

(a) Original signal
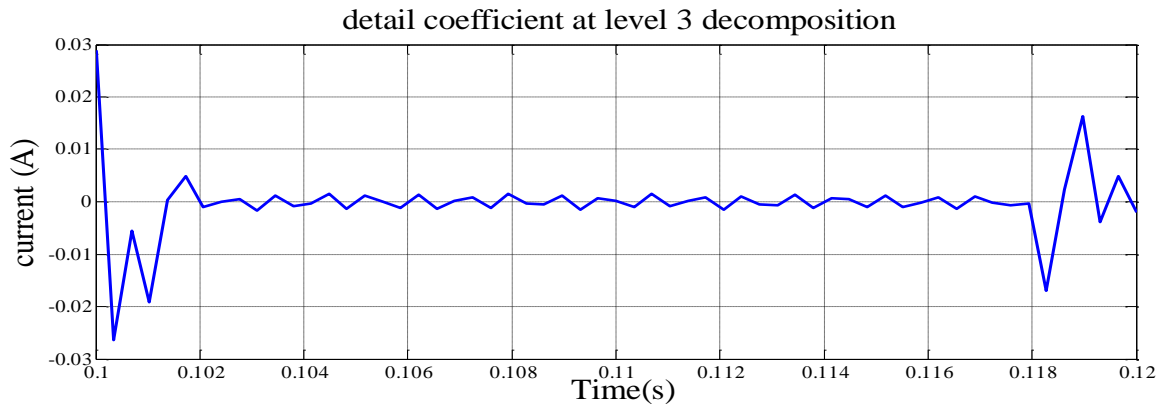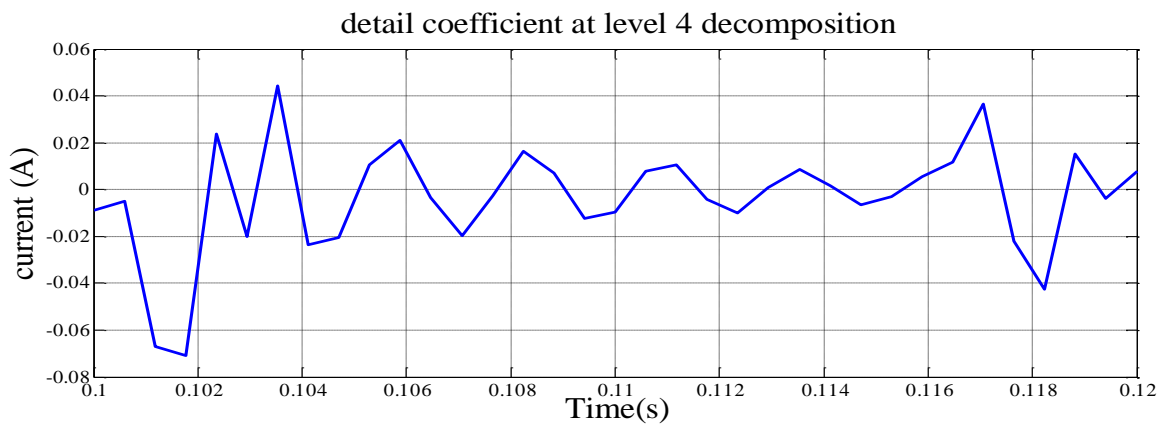
(b) Detail 1

(c) Detail 2

Fig. 5.2 Wavelet analysis of phase A differential current for normal case.

(a) Detail 3

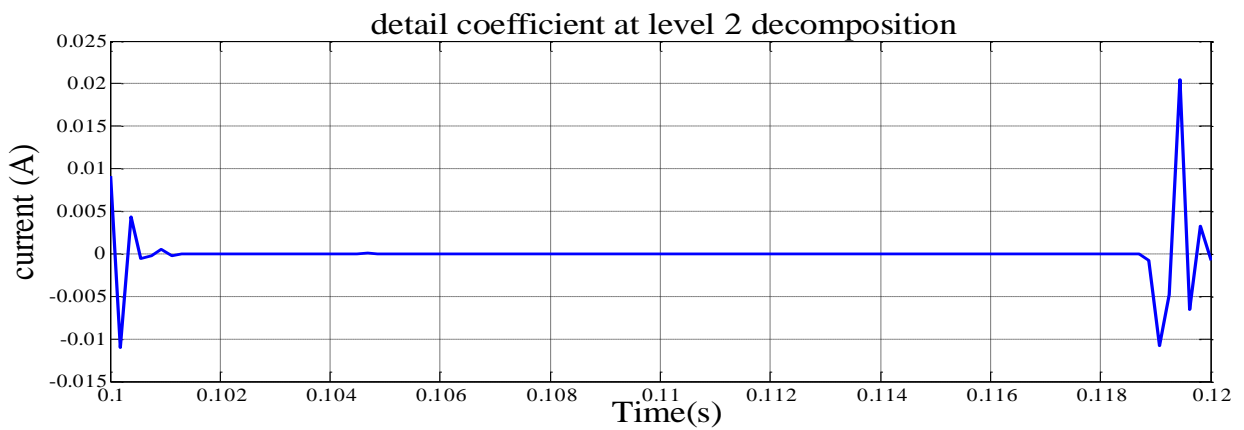(b) Detail 4

(c) Detail 5

5.3 Wavelet analysis in inrush case

Wavelet analysis for inrush case at the instant when switching takes place at 0^0 angle of the source voltage is shown in Fig 5.3 and 5.4. The Fig 5.3(a) represents the original current signal of phase A. It is seen that the current waveform is distorted in shape. Gaps appear over the times of inrush current. It is seen that the magnitude of inrush current changed from nearly zero value to a significant value at the edges of the gaps. This sudden change from one state to other should produce small ripples. But these ripples are not visible in the time domain representation. This phenomenon is clearly discriminated in the wavelet plots. The Fig 5.3 (b)-(c) and Fig 5.4 (a)-(c) represent the decomposed detail coefficient signals in different levels. From the figures of details it is clear that there are a number of sharp spikes during the period of the inrush current transient. High frequency component is located better in time domain and low frequency component is located better in frequency domain. Details 1 to 3 are located better in time domain as they contains high frequency components and detail 4 to 5 are located better in frequency domain as they contains low frequency components. The frequency bands of details 1 to 5 are given in Table 5.1.

Table 5.1: Frequency band of different detail coefficients

| Level of detail coefficient	Frequency band
d1	5 kHz-2.5 kHz
d2	2.5 kHz-1.25 kHz
d3	1.25 kHz-0.625 kHz
d4	0.625 kHz - 0.3125 kHz
d5	0.3125 kHz-0.15625 kHz
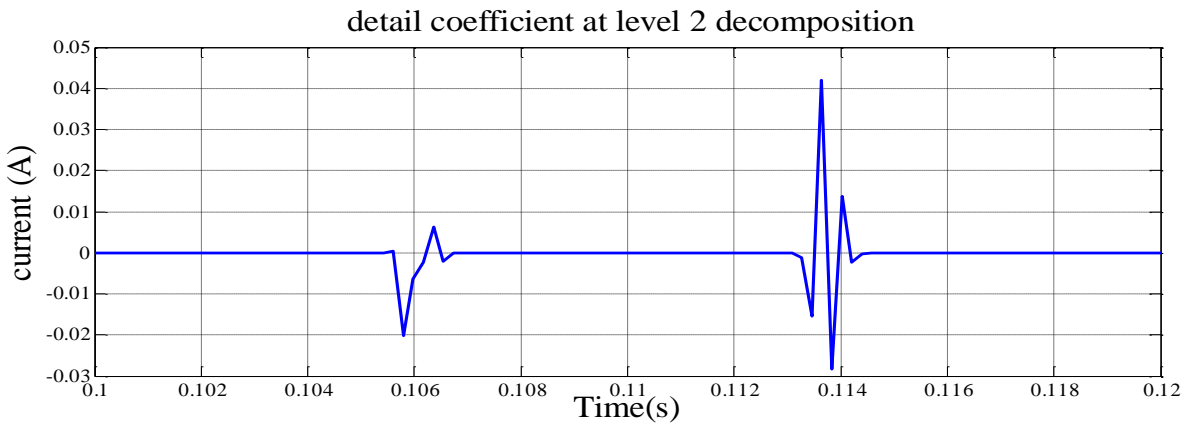
Fig. 5.3 Wavelet analysis of phase A differential current for inrush case.

(a) Original signal

(b) Detail 1

(c) Detail 2

detail coefficient at level 3 decomposition

(a)

detail coefficient at level 4 decomposition

(b)

detail coefficient at level 5 decomposition

(c)

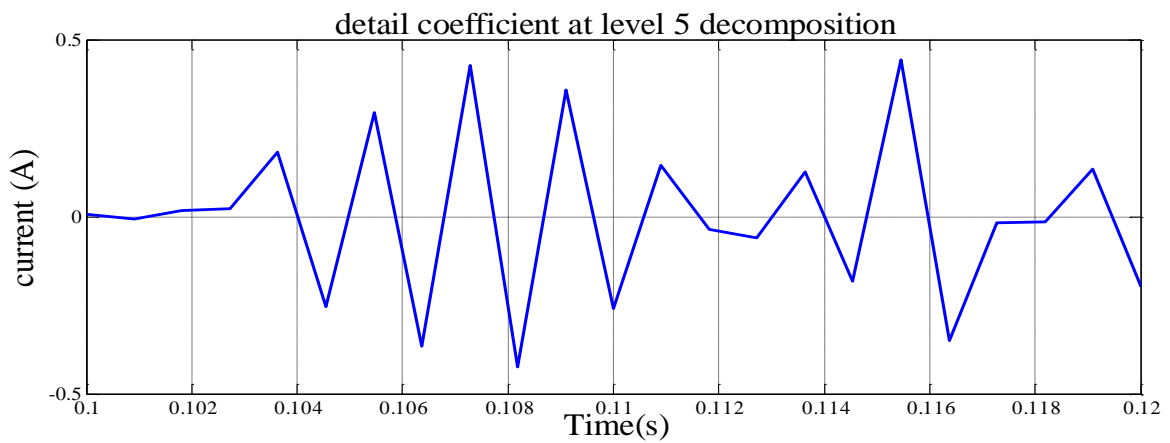Fig. 5.4 Wavelet analysis of phase A differential current for inrush case.

(a) Detail 3

(b) Detail 4

(c) Detail 5

5.4 Wavelet analysis in internal fault case

Wavelet analysis for internal fault case at the instant when switching takes place at 0^0 angle of the source voltage and 100Ω fault resistance for the time 0.1 to 0.12 seconds are shown in Fig 5.5 and 5.6. The Fig 5.5(a) represents the original current signal of phase A during L-G fault. The fault occurs on the high voltage side of power transformer. A high frequency distortion is observed in the fault current waveforms as shown in Fig 5.5 (a). This distortion is the consequence of the effects of distributed inductance and capacitance of the transmission line. This distributed inductance and capacitance lead to significant second harmonic in the internal fault during the transient period. Hence the distributed inductance and capacitance poses difficulty in an accurate discrimination between magnetizing inrush current and internal fault currents by the conventional protection method based on DFT. In the details 1-3 shown in Fig 5.5(b)-(c), and Fig 5.6 (a), it is observed that there are several spikes immediately after fault inception time in L-G fault. But these sharp spikes rapidly decay to zero within a cycle. But in inrush case these sharp spikes lasts in the entire inrush transient period. Details 1 to 3 are located better in time domain as they contains high frequency components and detail 4 to 5 are located better in frequency domain as they contains low frequency components. The figure 5.6 (b)-(c) represent the decomposed detail coefficient signals in different levels in L-G. Similar results are obtained for L-L-G fault, L-L-L-G fault, L-L and L-L-L-L fault cases. The frequency bands of details 1 to 5 are same as that of inrush case given in Table 5.1.
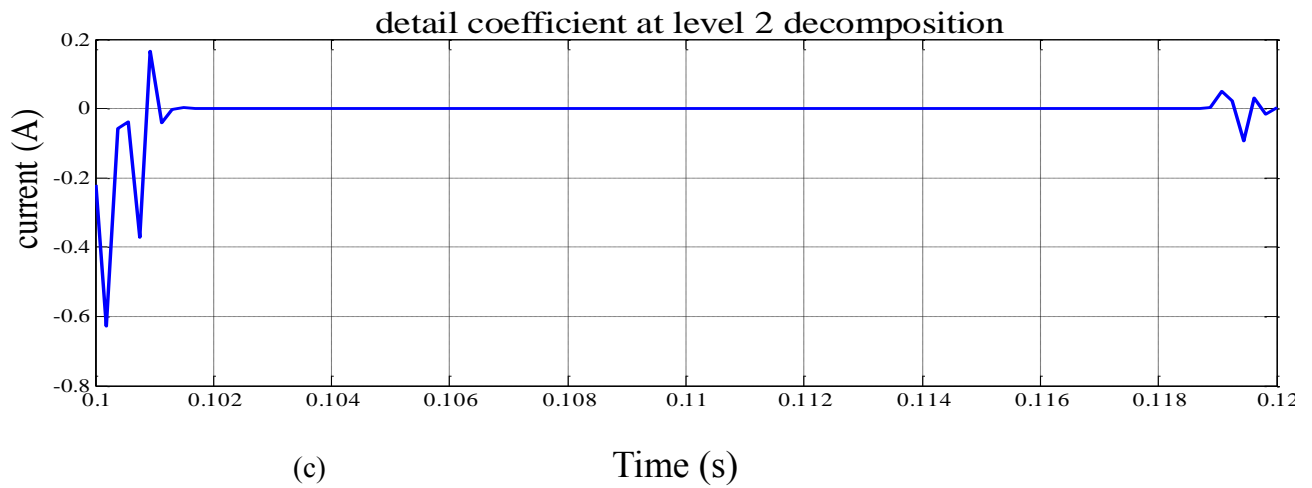
Fig. 5.5 Wavelet analysis of phase A differential current for L-G fault case.

(a) Original signal
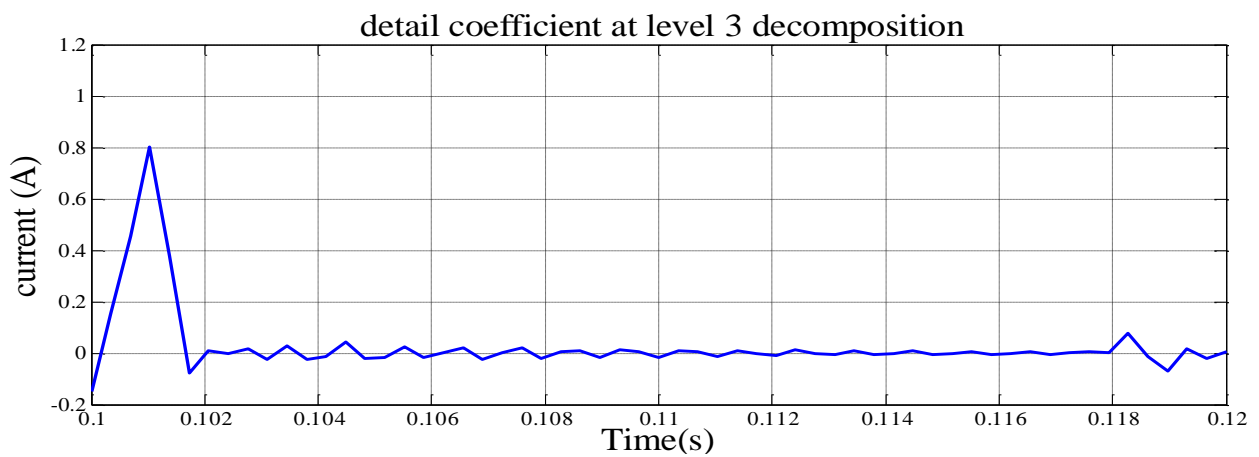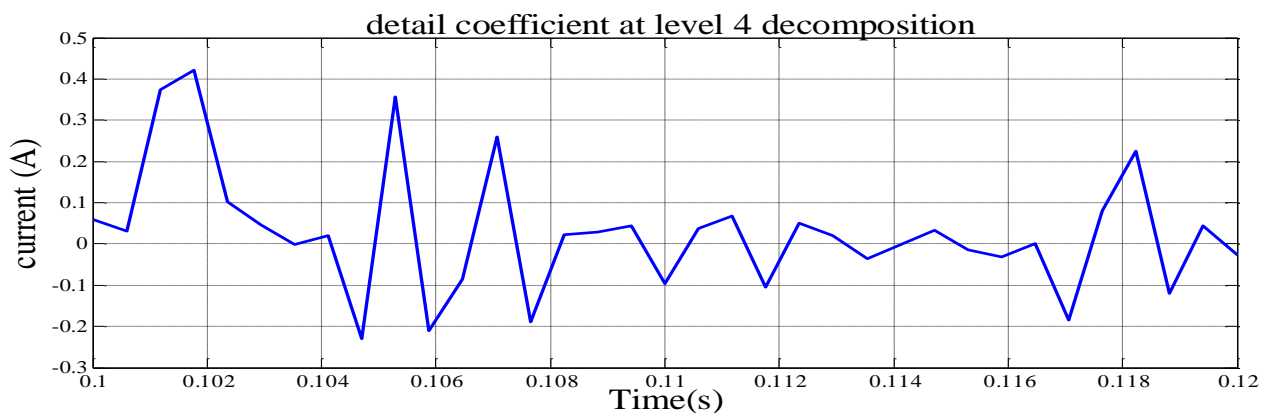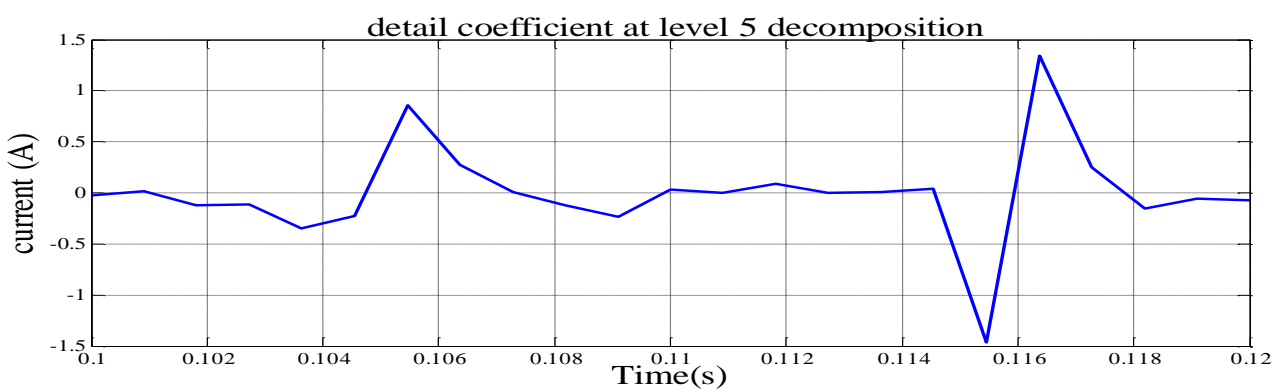
(b) Detail 1

(c) Detail 2

Fig. 5.6 Wavelet analysis of phase A differential current for L-G fault case.
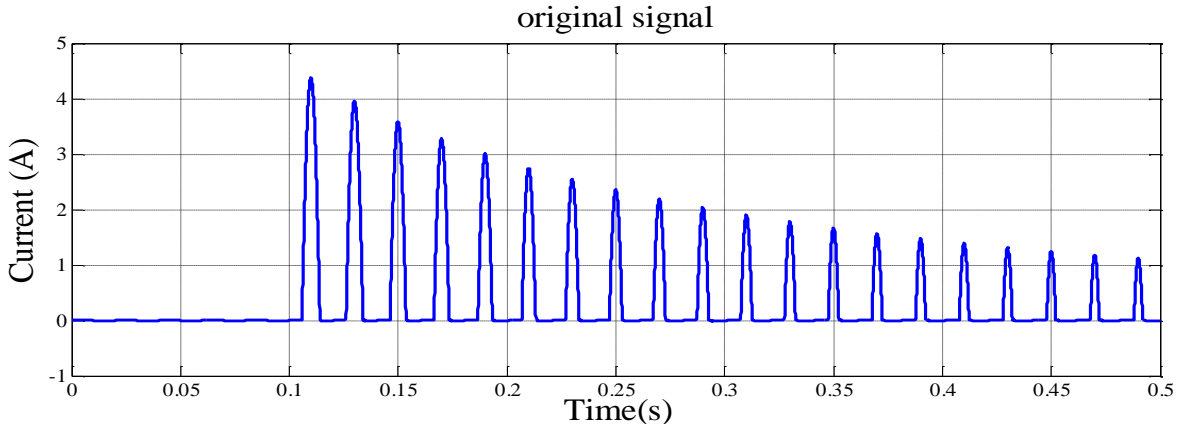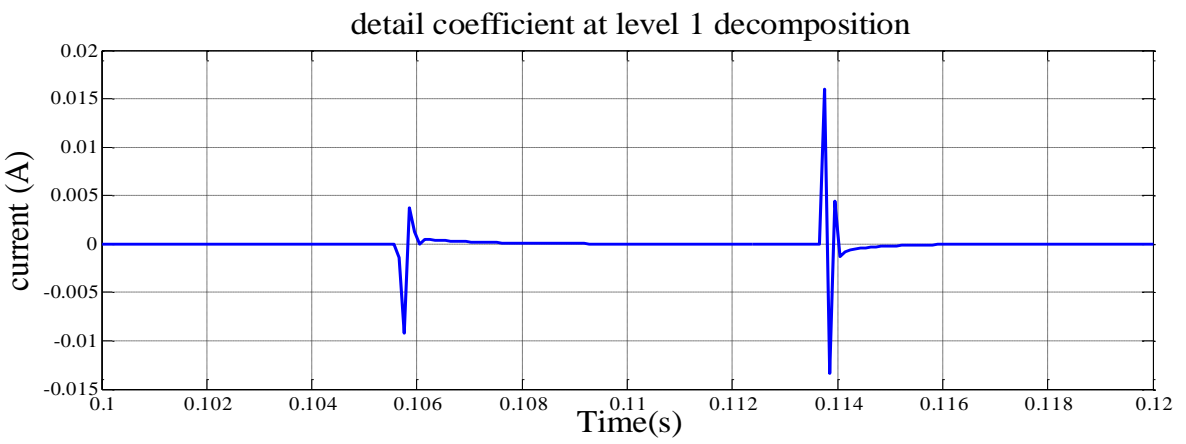
(a) Detail 3

(b) Detail 4

(c) Detail 5

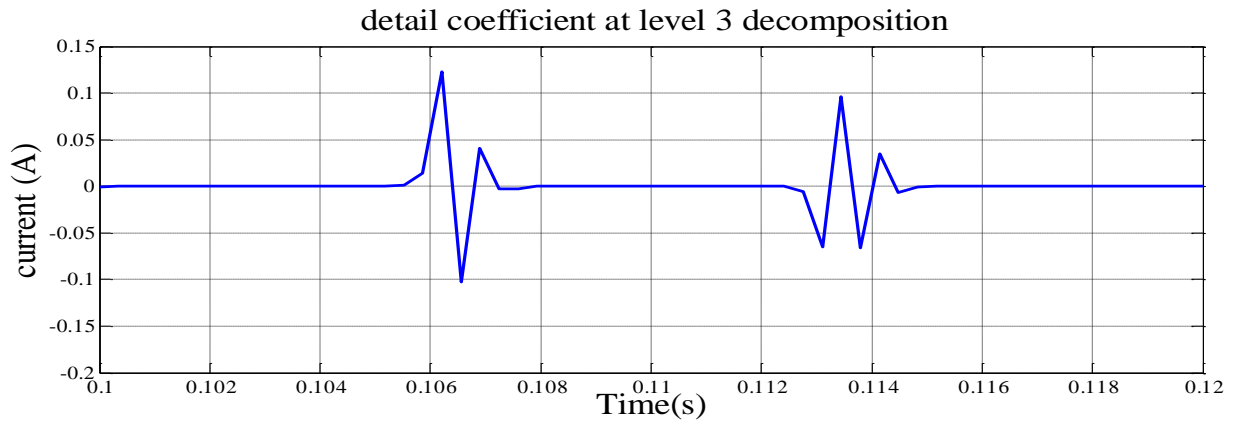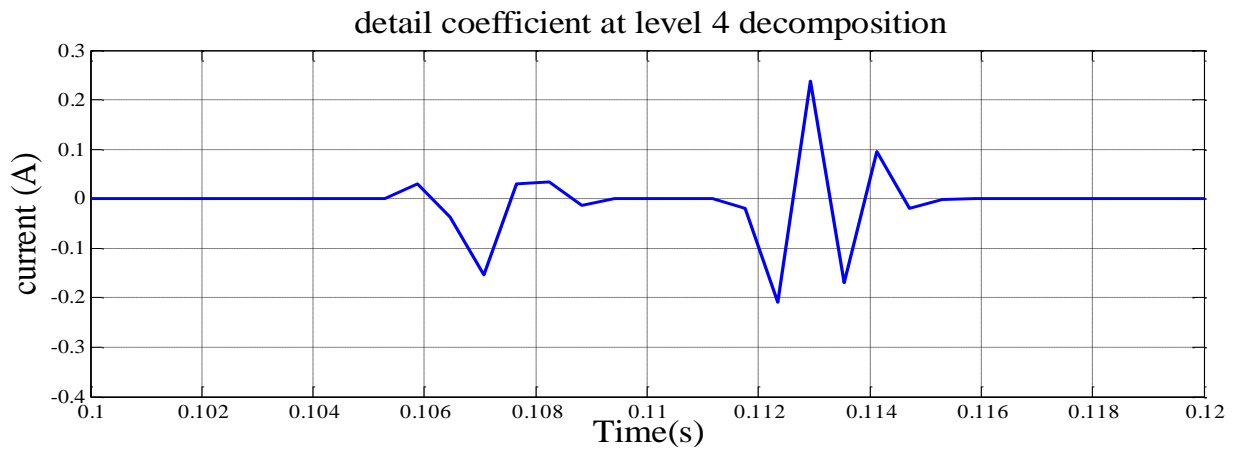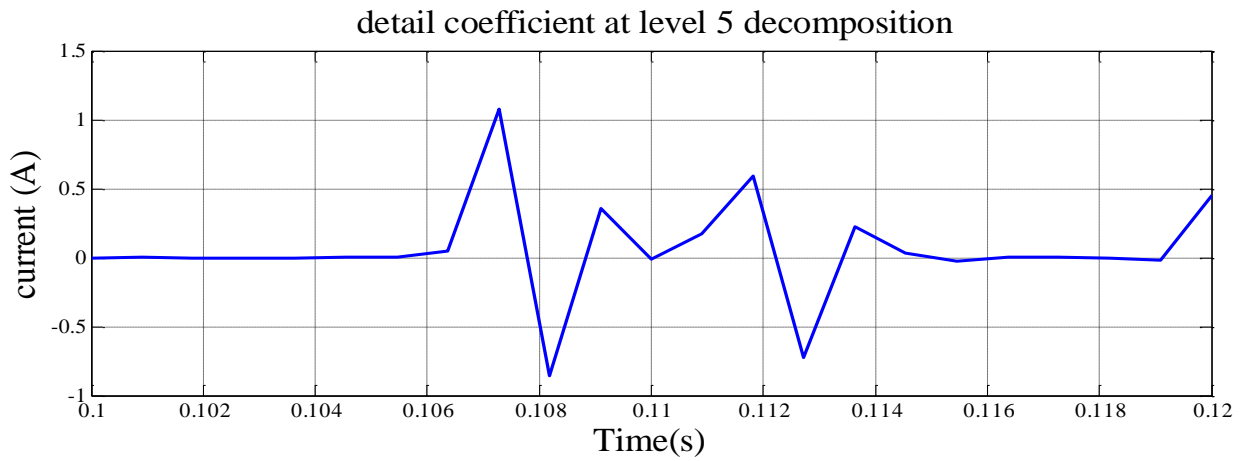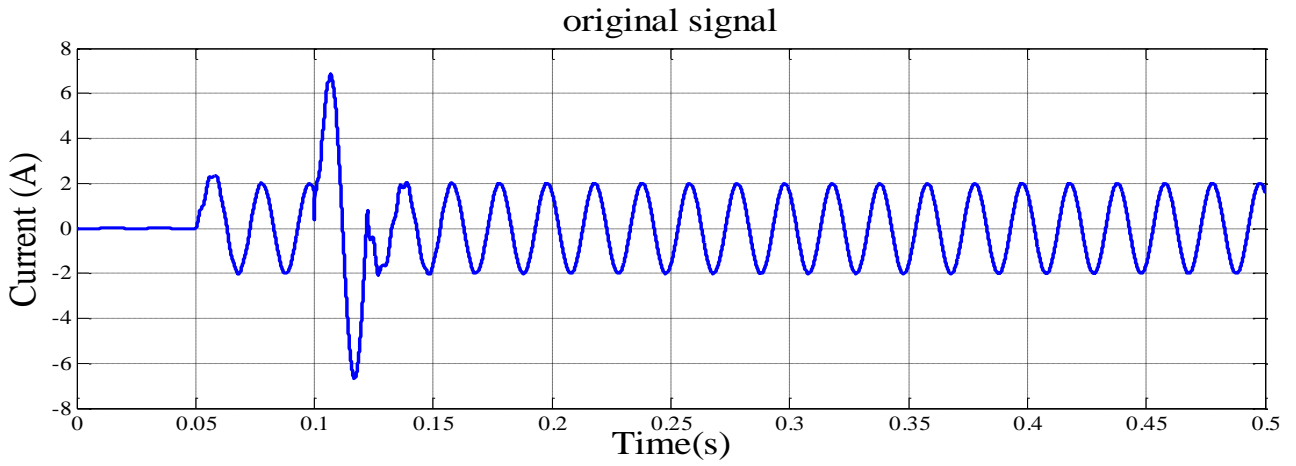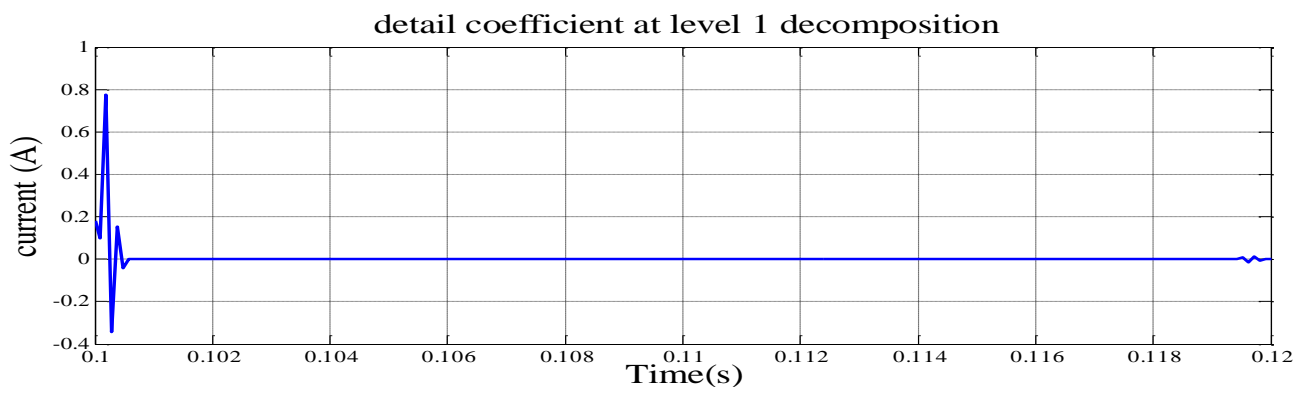# CHAPTER - 6

PERFORMANCE OF ANN

AND

IT'S IMPLEMENTATION IN LabVIEW

6.1 General method

The statistical data obtained from the decomposed signals of wavelet analysis at level 1 to 5 are used to train and test the ANN. Back propagation algorithm is used to train the ANN. The activation function used in the ANN is of sigmoid type. Similarly another one set of training data obtained for delta-star transformer (D11Y).The MATLAB code to extract the features from the transient signals is given in Appendix 3. During the formation of training data set the transformer is switched on at 0.1 sec for normal and inrush case, whereas at 0.05 sec for other cases. For normal and inrush cases the different pattern of data are generated by varying the phase angle of voltage. For fault cases the fault resistance is varied to generate different data. For over excitation case the value of the additional load is varied for generating different pattern of data.

The training and testing data are statistical features like mean, standard deviation and norm (root mean square value) of the decomposed detail coefficients in various levels. The data obtained after statistical analysis are normalized before training or testing by dividing the maximum value of data of a row with other data. The three type of statistical feature of each phase and similarly for three phases as a whole gives a row vector containing 9 data in each pattern during training and testing and are fed to the 9 input nodes of the ANN.

The ANN is trained and tested for each level decompose detail coefficients i.e. for high frequency and low frequency constituents and the detail comparison is given in Table 6.8 and Table 6.10 for star-star and delta-star transformer respectively. The architecture of the ANN having one hidden layer, 16 nodes in hidden layer, 9 nodes in input layer and 9 nodes in output layer is the best out of all the tested architecture as the mean square error in this type is least during training. The learning rate suitable for that network having least error is 0.2 and the momentum factor 0.9 in the same network gives the least error. The performance of ANN by varying the hidden layer nodes, learning rate and momentum factor are given in terms of mean square error in Table 6.1, Table 6.2 and table 6.3 respectively. The weights of the ANN after training using each level detail coefficient data are given for each level. The test results of the ANN using different detail levels are given in Table 6.9 and Table 6.11 for star-star and delta-star transformer respectively.

6.2 Performance of ANN using d1 level data for star-star transformer
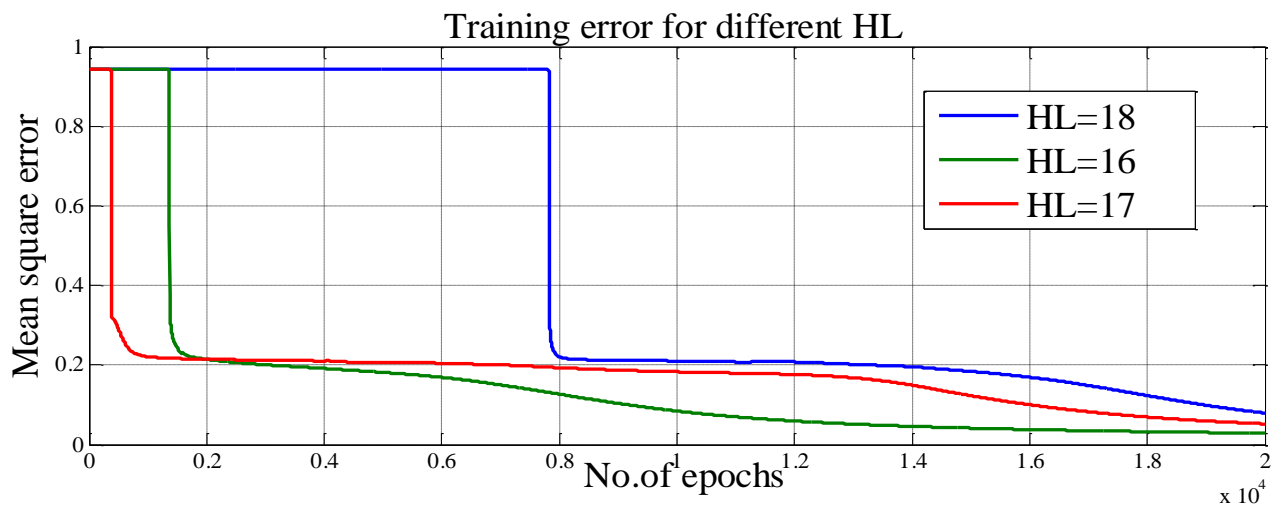
Fig. 6.1 Performance of ANN for different hidden layers.

The learning rate (n) and the momentum factor (m) are kept constant when the performance of ANN is checked for different hidden nodes (HL) in the hidden layer at 0.2 and 0.9 respectively. The least error is for HL=16.

Table: 6.1 Comparison of errors during training of ANN for different hidden layers

No. of HL	Mean square error during training after 20000 iterations
15	0.1677
16	**0.0288**
17	0.0522
18	0.0795
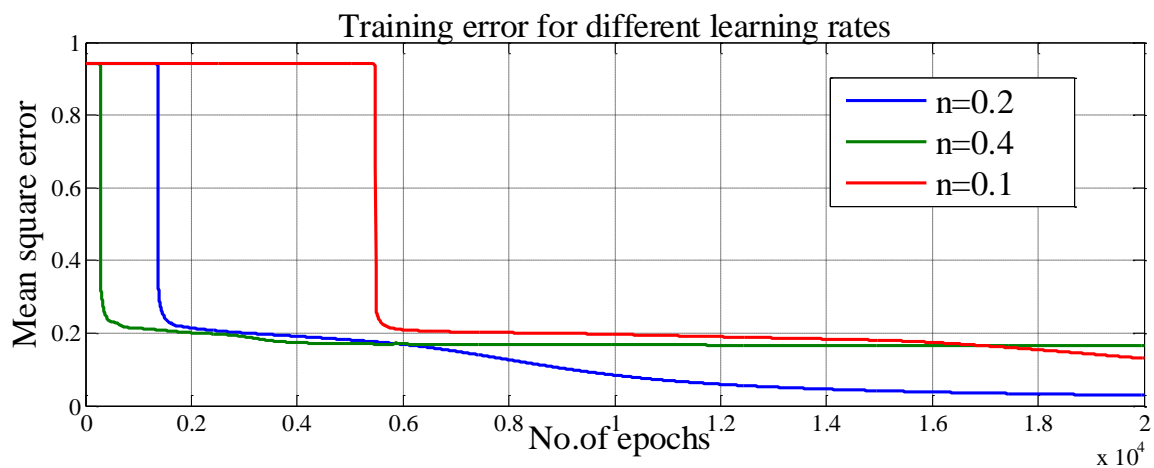
Fig. 6.2 Performance of ANN for different learning rates

The number of nodes in the hidden layer (HL) and the momentum factor (m) are kept constant when the performance of ANN is checked for different learning rates at 16 and 0.9 respectively. The least error is for n=0.2.

Table: 6.2 Comparison of errors during training of ANN for different learning rates

Learning rate (n)	Mean square error during training after 20000 iterations
0.1	0.1304
0.2	**0.0288**
0.4	0.1669
0.6	0.1668
0.8	0.1667
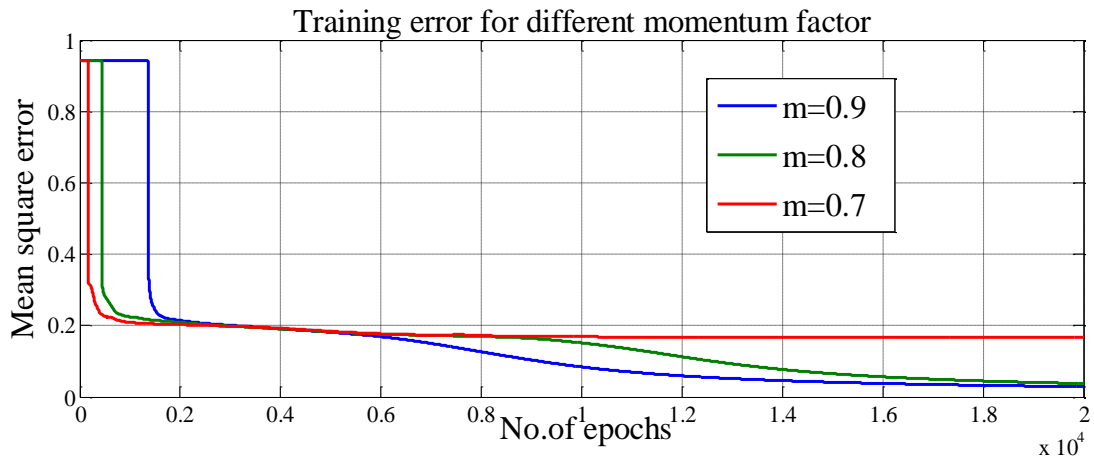
Fig. 6.3 Performance of ANN for different momentum factor

The number of nodes in the hidden layer (HL) and the learning rate (n) are kept constant when the performance of ANN is checked for different momentum factor at 16 and 0.2 respectively. The least error is for m=0.9.

Table: 6.3 Comparison of errors during training of ANN for different momentum factor

Momentum factor (m)	Mean square error during training after 20000 iterations
0.7	0.1671
0.8	0.0377
0.9	**0.0288**

Best suitable architecture of ANN

The ANN having 9 input nodes, 16 nodes in the hidden layer and 9 output nodes trained with learning rate equals to 0.2 and momentum factor equals to 0.9 is the best suitable one as it gives least mean square error during training.

Table- 6.4 Weights between input and hidden layer after training (Wa) Column 1 to 8

-4.4191	4.81626	1.47197	-0.0158	0.79443	1.3898	0.78116	-1.4926
1.09089	2.69956	0.41148	0.64326	0.98286	1.18898	-0.4468	-0.7386
9.4811	7.68751	-3.0176	-2.5147	9.86806	2.13751	-8.8081	-2.2395
14.7875	-30.141	0.49193	1.30116	-5.4159	2.22767	1.37414	16.5815
-2.6679	4.68341	1.81909	2.12887	-0.2267	0.85418	1.47997	-2.4525
0.43962	-6.3413	0.36504	5.79322	-17.72	2.63952	3.28631	-9.4502
-9.3934	27.4844	1.73863	1.45742	6.06712	-0.0889	0.15127	-11.651
-1.7439	5.16241	0.84197	1.32948	0.88546	-0.7326	0.70477	0.84743
-3.3464	4.01812	6.62588	4.64912	14.212	-10.684	2.15043	13.0464

Table- 6.5 Weights between input and hidden layer after training (Wa) Column 9 to 16

-2.2931	1.93121	0.5456	4.79095	2.05573	0.58412	1.70806	0.6143
0.79163	1.20983	1.70675	0.85903	1.11584	1.47794	1.59035	0.54692
-9.3422	-2.2498	9.12997	-2.4525	13.3731	18.876	0.51139	4.17639
10.7996	0.55699	2.37083	-15.726	-0.7939	-1.1624	-0.9381	1.94663
-3.1444	1.62985	-0.3429	5.95478	3.98855	6.76827	1.99057	1.20948
10.5048	1.42855	1.39299	-10.143	-14.818	-19.023	-2.515	4.20533
-5.1991	1.27706	0.62405	12.0287	2.65842	3.28515	1.0315	1.09173
-3.8511	0.41977	-0.9615	5.01609	4.4651	8.69261	1.68791	1.17475
-9.8472	6.42763	-12.61	11.5283	12.8714	16.1605	11.6916	1.62457

Table- 6.6 Weights between hidden and output layer after training (Wb)

-3.4312	-6.7524	0.18222	-3.293	-2.3979	1.19887	9.84708	-12.371	-1.1568
-2.1795	3.34862	1.12641	-1.7521	-20.322	0.39101	-21.732	13.9553	3.1549
0.56824	0.01419	-3.6086	-0.8468	-1.5322	-7.3313	2.17645	5.60559	1.72124
5.65037	-3.0843	-5.3623	0.86124	-3.8442	2.88033	-2.0495	1.02119	-2.233
2.07625	12.0365	2.44057	-6.8753	-14.114	2.00965	-10.216	-5.2946	-1.2285
-10.262	-5.065	-0.0197	0.24312	-3.5211	1.48463	-7.404	-3.0107	-5.7406
-8.8103	-3.8349	-1.032	3.49096	3.03122	-7.2106	-1.3142	4.80172	-7.3833
-15.286	1.60997	0.56085	-3.0204	3.80601	-2.0863	12.1505	-13.581	-3.8394
-7.8615	-11.777	-2.0746	2.03273	-8.6701	1.58737	6.84125	0.3774	1.8403
3.08936	-2.6637	-4.0528	2.34265	-4.2187	-3.4242	-0.3452	3.27995	0.99771
-0.9213	-11.208	1.55717	0.09589	-3.7918	3.70035	-9.108	-8.8431	10.894
-7.6421	5.52669	1.07521	-2.3521	8.96134	-2.6221	-16.725	7.92746	-2.4494
4.13038	6.72747	2.81986	-4.1789	5.71471	-5.5134	-8.0204	-10.088	-9.4337
7.98779	8.0395	0.56585	-5.5737	13.7031	-2.1941	-5.4052	-13.363	-9.9948
6.35174	-5.6023	-1.0597	-3.259	-3.0732	-5.4576	6.24367	4.37069	8.03665
-5.7974	-9.037	-1.6488	-0.2295	-4.078	-1.2669	-2.9179	0.31194	-4.0435

Table- 6.7 Test results using d1 level data for star-star transformer

Normal	Inrush	L-G	L-L-G	L-L-L-G	L-L	L-L-L	EF	OE
0.011383	1.96E-08	1.01E-06	8.20E-05	4.10E-06	6.10E-12	0.000199	0.0704344	1.06E-07
0.80022	5.86E-11	6.32E-07	0.000271	1.68E-09	4.72E-10	0.000607	0.2980568	2.81E-05
0.792538	2.67E-13	0.000293	2.48E-06	1.28E-12	0.000182	4.67E-15	8.68E-10	0.001931
0.999995	0.00016	0.008793	1.17E-10	1.10E-16	1.15E-05	7.37E-20	6.52E-12	0.001714
0.008096	0.999221	0.002112	6.23E-13	2.04E-10	2.83E-10	8.23E-18	7.23E-10	2.35E-08
0.000746	0.834766	0.058545	4.96E-13	1.11E-10	7.90E-09	4.44E-20	7.28E-13	1.40E-05
0.002465	0.999958	0.000774	1.81E-12	1.37E-09	1.30E-11	2.28E-17	1.27E-07	2.97E-10
7.51E-05	0.999993	0.000236	5.20E-10	3.24E-06	2.08E-14	1.78E-19	0.009171	1.89E-12
0.011588	0.007819	0.99577	3.92E-11	9.01E-14	0.007338	8.57E-23	5.30E-16	5.09E-06
0.012215	0.007658	0.9958	4.08E-11	8.33E-14	0.008114	1.11E-22	4.31E-16	4.97E-06
0.012683	0.00755	0.995755	4.12E-11	8.11E-14	0.008204	1.16E-22	4.25E-16	5.00E-06
0.014792	0.007018	0.995504	4.19E-11	7.38E-14	0.008119	1.23E-22	4.48E-16	5.27E-06
3.33E-12	1.23E-22	9.07E-07	0.990523	2.02E-12	0.004978	0.008566	0.0001759	0.003457
4.54E-12	1.53E-22	1.03E-06	0.991229	2.01E-12	0.006286	0.004356	0.0002523	0.005065
4.72E-12	1.58E-22	1.05E-06	0.991283	2.00E-12	0.006556	0.00399	0.0002618	0.005308
4.78E-12	1.56E-22	1.07E-06	0.99119	1.97E-12	0.006764	0.003934	0.0002536	0.00548
1.64E-06	0.000205	3.17E-06	5.53E-06	0.996526	4.85E-14	0.000103	7.11E-05	4.98E-11
3.40E-06	0.040758	8.33E-06	1.18E-06	0.932659	2.35E-14	1.57E-09	0.0066855	2.83E-11
3.24E-06	0.059852	9.07E-06	1.06E-06	0.840454	2.34E-14	3.83E-10	0.0160617	3.30E-11
3.72E-06	0.093609	1.01E-05	8.32E-07	0.782042	2.23E-14	1.64E-10	0.0169277	2.87E-11
1.78E-07	1.25E-17	0.000838	0.00556	4.48E-13	0.991299	8.58E-10	1.27E-10	0.006388
3.81E-07	1.49E-16	0.001393	0.001778	4.47E-15	0.985134	4.65E-13	3.39E-09	0.007241
4.19E-07	1.88E-16	0.001459	0.00162	3.29E-15	0.984326	2.60E-13	4.34E-09	0.007298
4.48E-07	2.05E-16	0.001472	0.001553	3.12E-15	0.983681	2.19E-13	4.54E-09	0.00719
3.09E-08	9.62E-14	9.75E-08	0.004295	1.41E-05	3.26E-11	1	4.73E-05	3.39E-06
1.16E-05	1.22E-10	2.92E-07	0.001128	5.49E-05	9.50E-12	0.980221	0.018569	6.82E-07
3.74E-05	1.44E-10	2.98E-07	0.001524	6.92E-06	1.32E-11	0.720706	0.2627186	1.72E-06
3.07E-05	3.37E-13	8.93E-08	0.042976	9.22E-09	1.53E-10	0.988252	0.9971715	0.000384
7.11E-06	9.16E-10	3.50E-07	0.002024	4.99E-06	7.64E-12	0.022665	0.9674923	2.64E-06
3.96E-05	2.24E-10	2.96E-07	0.002702	8.00E-07	1.56E-11	0.057998	0.9660648	5.81E-06
0.011006	3.43E-11	2.99E-07	0.001789	2.17E-08	7.67E-11	0.043967	0.8848975	1.48E-05
0.758565	2.02E-15	4.06E-06	0.000133	2.50E-13	2.66E-06	7.12E-08	9.56E-05	0.575438
0.013342	2.76E-18	1.78E-06	0.002577	1.81E-15	3.38E-05	4.96E-06	0.003239	0.988715
0.011309	2.25E-18	1.97E-06	0.002465	1.44E-15	4.62E-05	3.16E-06	0.0023189	0.989743
0.019571	5.00E-18	1.40E-06	0.002851	3.35E-15	1.55E-05	1.49E-05	0.007458	0.983775
0.066952	2.12E-16	5.67E-07	0.003873	7.70E-14	5.46E-07	0.001225	0.2327961	0.699722

The red marked cases are correct identification and the green marked cases are incorrect identification in the Table 6.7.

Table: 6.8 Comparison of training error for different wavelet decomposition level

Wavelet decomposition level	Training error for different output nodes with HL=16, n=0.2 and m=0.9 after 30000 iterations								
	Node 1	Node 2	Node 3	Node 4	Node 5	Node 6	Node 7	Node 8	Node 9
d1	.1668	.0112	.0037	.0024	.0219	.0040	.0185	.0153	.0087
d2	.0215	.0086	.0026	.0036	.1713	.0037	.2445	.0130	.0075
d3	.1685	.0045	.0036	.0035	.1855	.0069	.1943	.0141	.0087
d4	.1724	.1684	.0047	.0531	.0480	.0317	.1164	.0083	.0120
d5	.1668	.2357	.0045	.0133	.0247	.0071	.0424	.0165	.0098

Table: 6.9 Comparison of test results of ANN for different wavelet decomposition level

Name of the event	% of correct discrimination using different wavelet decomposition level data for training after 30000 iterations and for HL=16,n=0.2,m=0.9				
	d1	d2	d3	d4	d5
Normal operating condition	75	**100**	25	0	50
Inrush condition	**100**	50	**100**	75	25
Internal L-G fault	**100**	**100**	**100**	**100**	**100**
Internal L-L-G fault	**100**	**100**	**100**	**100**	**100**
Internal L-L-L-G fault	**100**	**100**	**100**	50	**100**
Internal L-L fault	**100**	**100**	**100**	50	75
Internal L-L-L fault	75	25	25	75	75
External L-L-L-G fault	75	75	**100**	**100**	75
Over excitation condition	**100**	**100**	**100**	**100**	**100**

6.3 Performance of ANN with d1 level data for delta- star transformer

**Table: 6.10 Comparison of training error for different wavelet decomposition level**

Wavelet decomposition level	Training error for different output nodes with HL=16, n=0.2 and m=0.9 after 20000 iterations								
	Node 1	Node 2	Node 3	Node 4	Node 5	Node 6	Node 7	Node 8	Node 9
d1	.1673	.0097	.0051	.0036	.2240	.0046	.2265	.0079	.0144
d2	.1677	.0094	.0065	.0082	.2195	.0056	.2186	.0124	.0441
d3	.0738	.0153	.0048	.0088	.2184	.0103	.2104	.0101	.0179
d4	.0612	.0416	.0023	.0015	.0926	.0402	.1903	.0245	.0136
d5	.1103	.0617	.0231	.0026	.1328	.0824	.1304	.0340	.0127

Table: 6.11 Comparison of test results of ANN for different wavelet decomposition level

Name of the event	% of correct discrimination using different wavelet decomposition level data for training after 20000 iterations and for HL=16,n=0.2,m=0.9				
	d1	d2	d3	d4	d5
Normal operating condition	75	**75**	75	25	75
Inrush condition	**100**	75	**100**	75	**100**
Internal L-G fault	**100**	**100**	**100**	**100**	**100**
Internal L-L-G fault	**100**	**100**	50	**100**	**100**
Internal L-L-L-G fault	0	50	**100**	75	**100**
Internal L-L fault	**100**	**100**	**100**	75	50
Internal L-L-L fault	**100**	75	25	75	75
External L-L-L-G fault	75	75	**100**	**100**	75
Over excitation condition	**100**	**100**	**100**	**100**	**100**

6.4 LabVIEW implementation of the ANN

After the proper training of ANN the weights obtained are used in the testing of ANN in LabVIEW environment. The results obtained using the d1 level analysis for star-star transformer using the weights given in Table 6.4- 6.6 are given in Fig 6.4 and Fig 6.5. The structure of the implementation is given in Appendix 4.
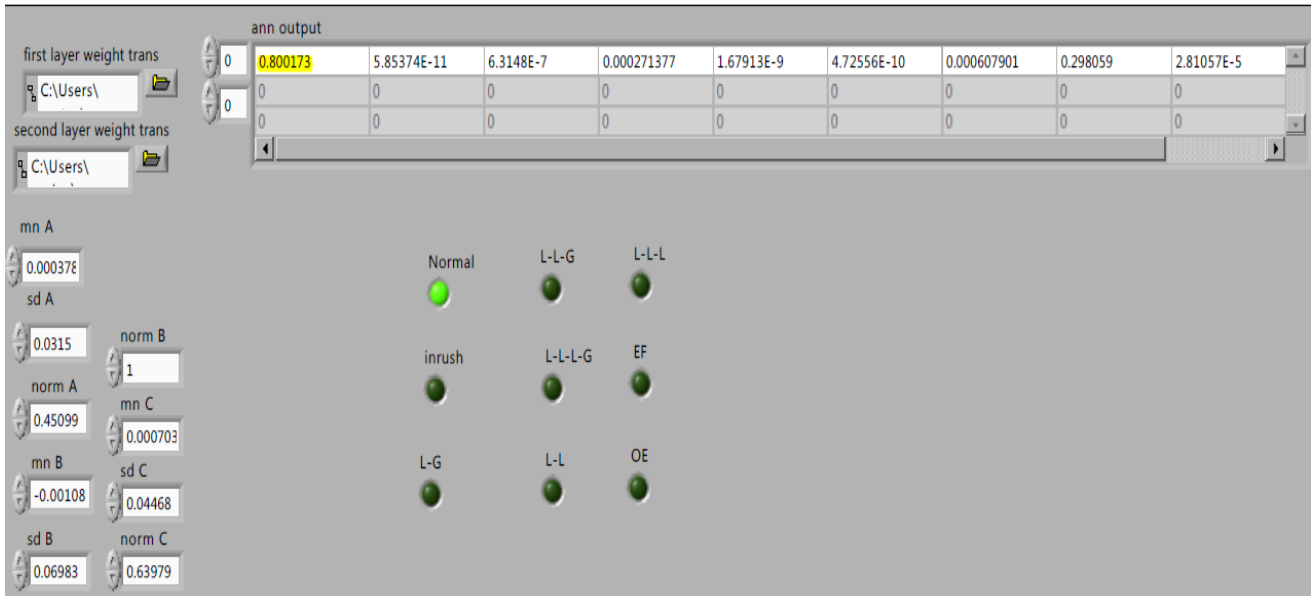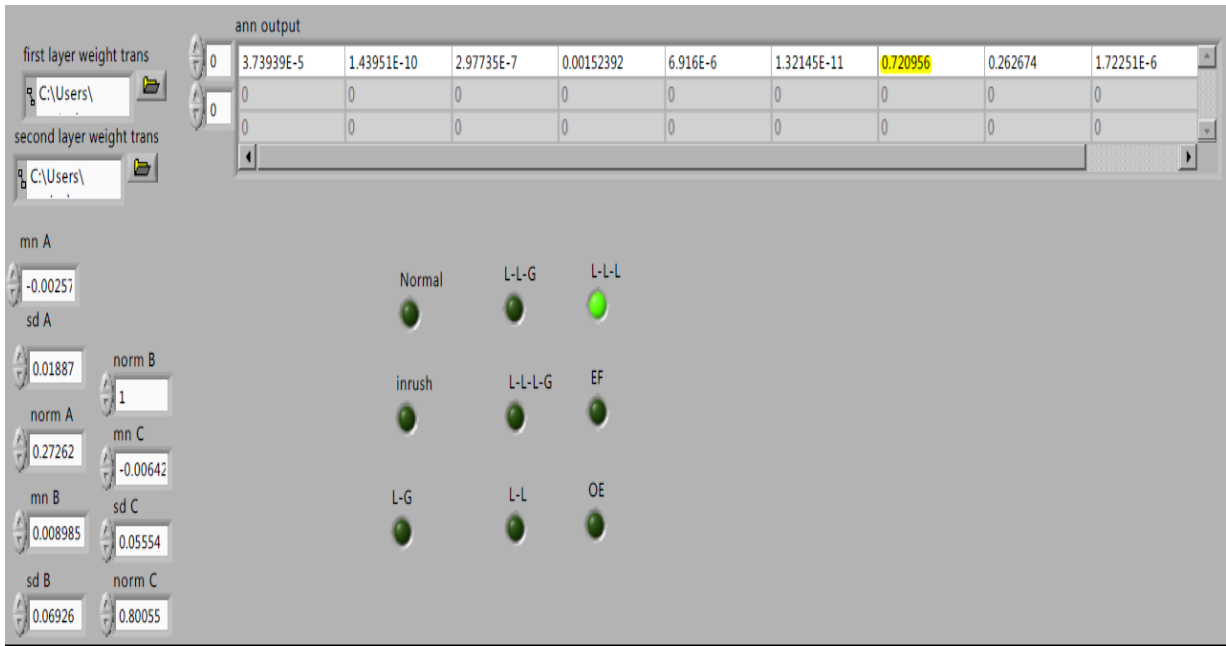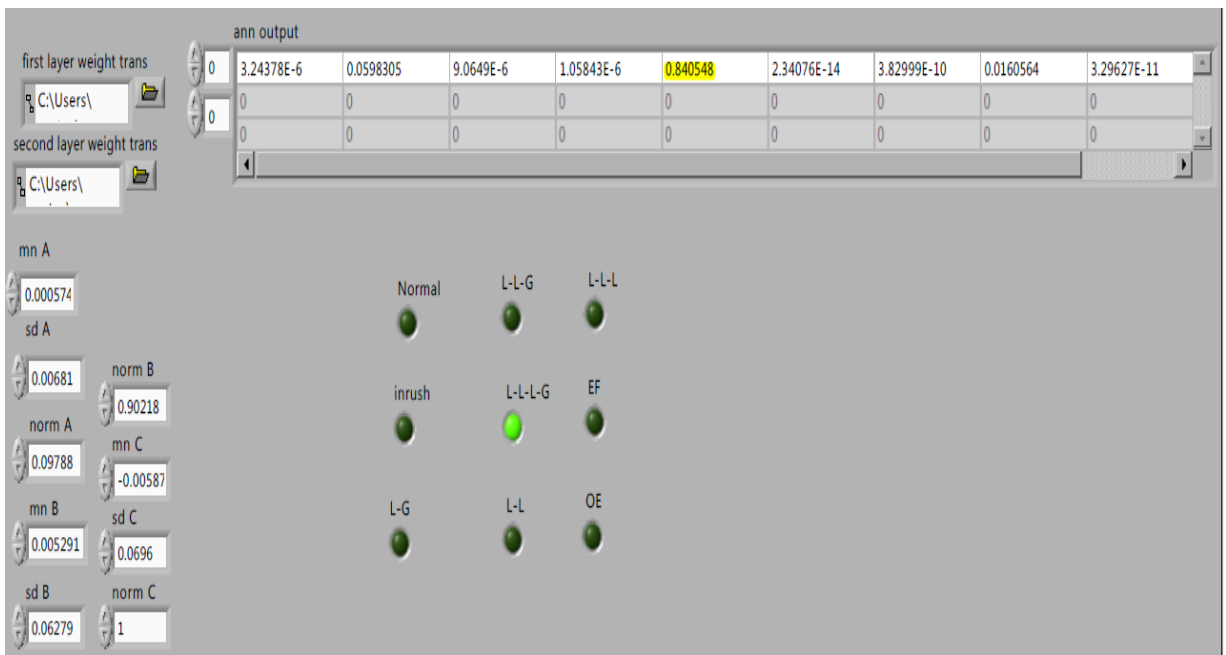

(a)
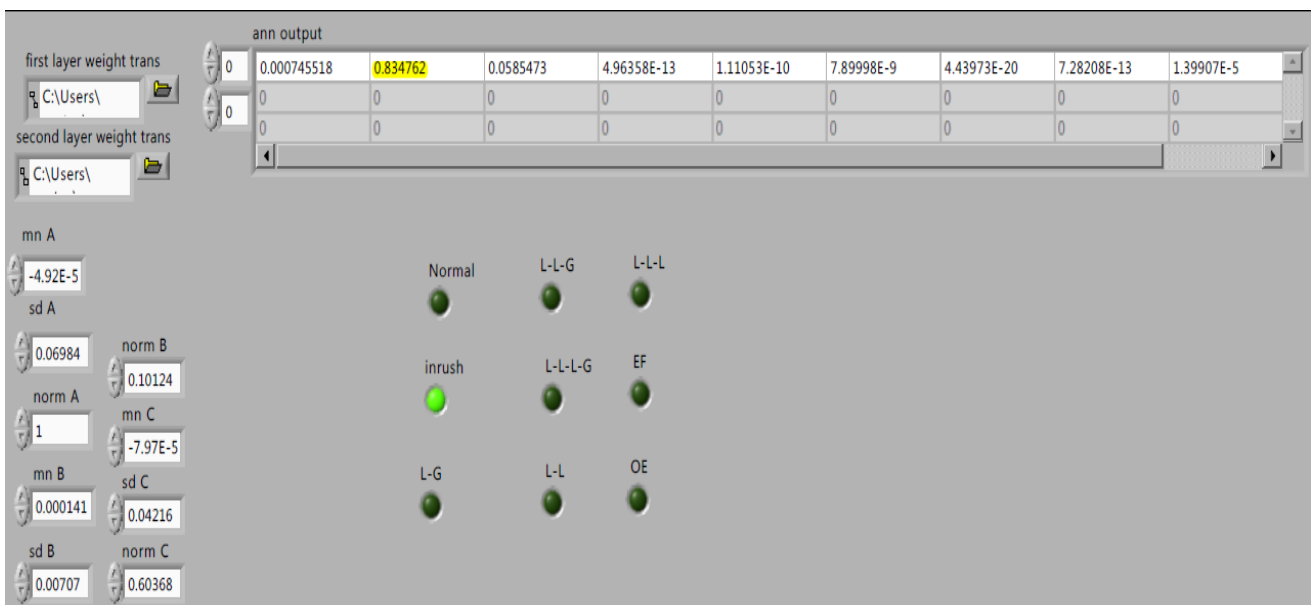
(b)

Fig 6.4 Detection of normal and inrush case

(a) Normal

(b) Inrush

51

(a)

(b)

Fig 6.5 Detection of L-L-L and L-L-L-G fault

(a) L-L-L fault

(b) L-L-L-G fault

CHAPTER – 7
GENERAL CONCLUSIONS
AND
SCOPE FOR FUTURE WORK

7.1 Conclusion

The current signals for different cases for a power transformer are obtained using MATLAB/SIMULINK. These waveforms are analysed using wavelet transform for extraction of feature vector (containing statistical data) to train the ANN. The performance of trained ANN is tested successfully for the classification of various cases. ANN is implemented in the LabVIEW environment for real time application.

From the study and analysis carried out in this dissertation, the performance of neural networks has been found to surpass the performance of conventional methods, which need accurate sensing devices, costly equipment and an expert operator or engineer.

The classification ability of the ANN in combination with advanced signal processing technique opens the door for smart relays for power transformer protection with very less operating time and with desirable accuracy.

7.2 Future scope

- Prototype modelling based on ANN and WT for protection of power transformer.
- Online testing of the algorithm.
- Comparison of ANN with other classifier like support vector machine (SVM).
- Analysis of performance of WT in noisy environment.
- Application of S transform in combination with ANN for transformer protection

REFERENCES

[1] P.L.Mao and R.K.Aggarwal. "A wavelet transform based decision making logic method for discrimination between internal faults and inrush currents in power transformers" International journal of Electric power and Energy systems, Vol.22, no.6, 389-395.Oct 2000.

[2] Symon Haykin. "A text book on Neural Networks", 2nd ed. Prentice Hall:1998

[3] S. N. Deepa, S.S.Sumathi, S.N.Sivanandam. "Neural Network using MATLAB", 1st ed.Tata Mcgraw Hill:2009.

[4] M. Tripathy, R.P. Maheshwari, H.K. Verma, "Advances in transformer protection: a review", Electric Power Compo. Syst. 33 (11) 1203–1209 2005.

[5] P. Arboleya, G. Diaz, J.G. Aleixandre, "A solution to the dilemma inrush/fault in transformer relaying using MRA and wavelets", Electric Power Compo. Syst. 34 (3) 285–301, 2006.

[6] H.K. Verma, G.C. Kakoti, "Algorithm for harmonic restraint differential relaying based on the discrete Hartley transform", Electric Power Syst. Res. 18 (2) , 125–129, 1990.

[7] M.C. Shin, C.W. Park, J.H. Kim, "Fuzzy logic based relaying for large power transformer protection", *IEEE Transactions on Power Delivery*. 18 (3),718–724, 2003.

[8] S.A. Saleh, M.A. Rahman, "Modeling and protection of a three-phase transformer using wavelet packet transform", *IEEE Transactions on Power Delivery*. 20 (2),1273–1282, 2005.

[9] G. Diaz, P. Arboleya, J.G. Aleixandre, "A new transformer differential protection approach on the basis of space-vectors examination", Electrical Engg. 87,129–135, 2005.

[10] B. He, X. Zhang, Z.Q. Bo, "A new method to identify inrush current based on error estimation", *IEEE Transactions on Power Delivey*. 21 (3),1163–1168, 2006.

[11] E. Vazquez, I.I. Mijares, O.L. Chacon, A. Conde, "Transformer differential protection using principal component analysis", *IEEE Transactions on Power Delivey*.23 (1), 67–72, 2008.

[12] X.N. Lin, P. Liu, O.P. Malik, "Studies for identification of the inrush based on improved correlation algorithm", *IEEE Transactions on Power Delivery*. 17 (4), 901–907, 2002.

[13] K. Yabe, "Power differential method for discrimination between fault and magnetizing inrush current in transformers", *IEEE Transactions on Power Delivery*. 12 (3), 1109–1118, 1997.

[14] L. Yongli, H. Jiali, D. Yuqian, "Application of neural network to microprocessor based transformer protective relaying", *IEEE Int. Conf. on Energy Management and Power Delivery*, vol. 2, 21–23, pp. 680–683, November 1995.

[15] L.G. Perez, A.J. Flechsing, J.L. Meador, Z. Obradovic, "Training an artificial neural network to discriminate between magnetizing inrush and internal faults", *IEEE Transactions on Power Delivery*. 9 (1), 434–441, 1994.

[16] P. Bastard, M. Meunier, H. Regal, "Neural network based algorithm for power transformer differential relays", *IEE Proceedings Generation. Transmission and Distribution*. 142 (4), 386–392, 1995.

[17] J. Pihler, B. Grcar, D. Dolinar, "Improved operation of power transformer protection using artificial neural network", *IEEE Transactions on Power Delivery*. 12 (3),1128–1136, 1997.

[18] M.R. Zaman, M.A. Rahman, "Experimental testing of the artificial neural network based protection of power transformers", *IEEE Transactions on Power Delivery*. 13 (2), 510–517, 1998.

[19] A.L.Orille-Fernandez,N.K.I.Ghonaim, J.A.Valencia, "A FIRANN as differential relay for three phase power transformer protection", *IEEE Transactions on Power Delivery*.16 (2),215-218, 2001.

[20] H. Khorashadi-Zadeh, "Power transformer differential protection scheme based on symmetrical component and artificial neural network", *IEEE Int. Conf. on Neural Network Application in Electrical Engineering*, 23–25, pp. 680–683, September, 2004.

[21] Z. Moravej, "Evolving neural nets for protection and condition monitoring of power transformer", Electric Power Compo. Syst. 33 (11), 1229–1236, 2005.

[22] W. A. Wilkinson and M. D. Cox, "Discrete wavelet analysis of power system transients," *IEEE Trans. Power System*, vol. 11, no. 4, pp. 2038–2044, Nov. 1996.

[23] G. T. Heydt and A. W. Galli, "Transient power quality problems analysed using wavelets," *IEEE Trans. Power Delivery*, vol. 12, no. 2, pp. 908–915, Apr. 1997.

[24] S. K. Pandey and L. Satish, "Multiresolution signal decomposition: A new tool for fault detection in power transformers during impulse tests," *IEEE Trans. Power Delivery*, vol. 13, no. 4, pp. 1194–1200, Oct. 1998.

APPENDIX-1

POWER SYSTEM SPECIFICATION

Source

Three phase, star connected (Yg), 230 kV, 50 Hz

Source resistance (Rs=0.8929Ω)

Source inductance (Ls = 16.58e-3H)

Transformer

450 MVA, 50Hz, star-star

LV winding:

230kV, resistance=0.02p.u, inductance= 0.08 p.u

HV winding:

500kV, resistance=0.02p.u, inductance= 0.08 p.u

Transmission line

Length= 100 km

Resistance/km=0.01273Ω

Inductance/km=0.9337e-3H

Capacitance/km=12.04e-9 F

Load

450MW, 530MVAR

Primary CT ratio

3000/5

Secondary CT ratio

800/5

APPENDIX – 2
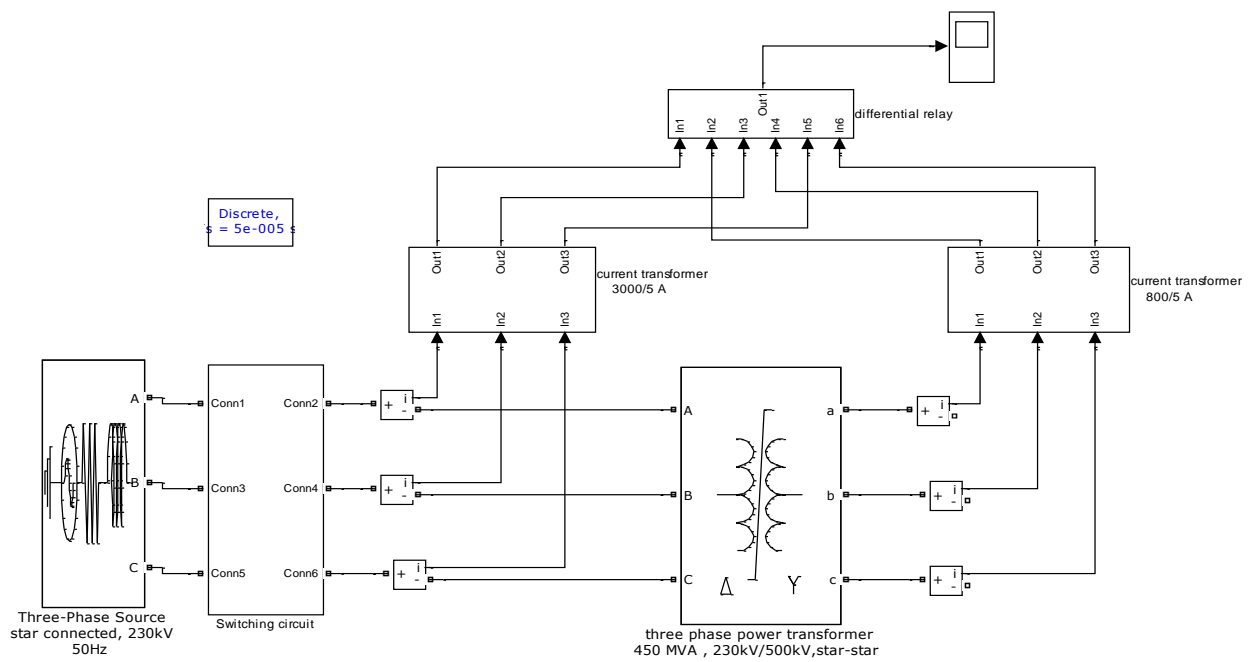# SIMULINK DIAGRAMS

Inrush condition

Fig. A 2.1 Inrush condition

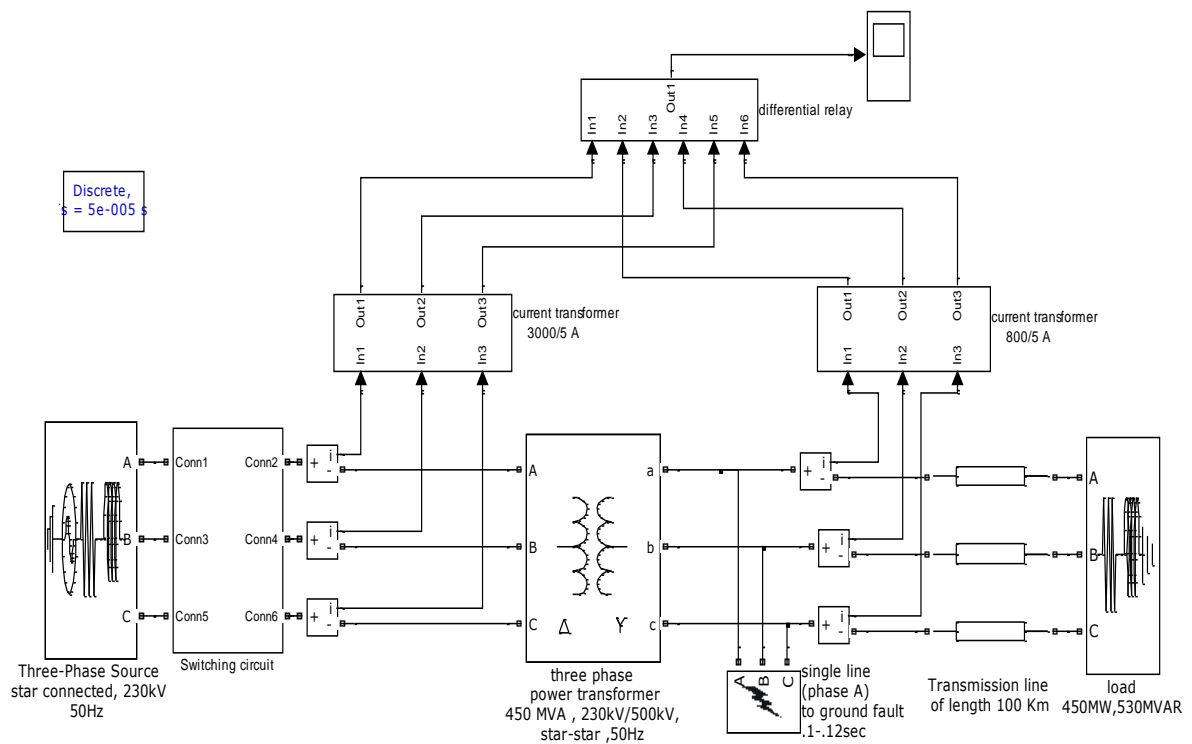# Internal fault condition

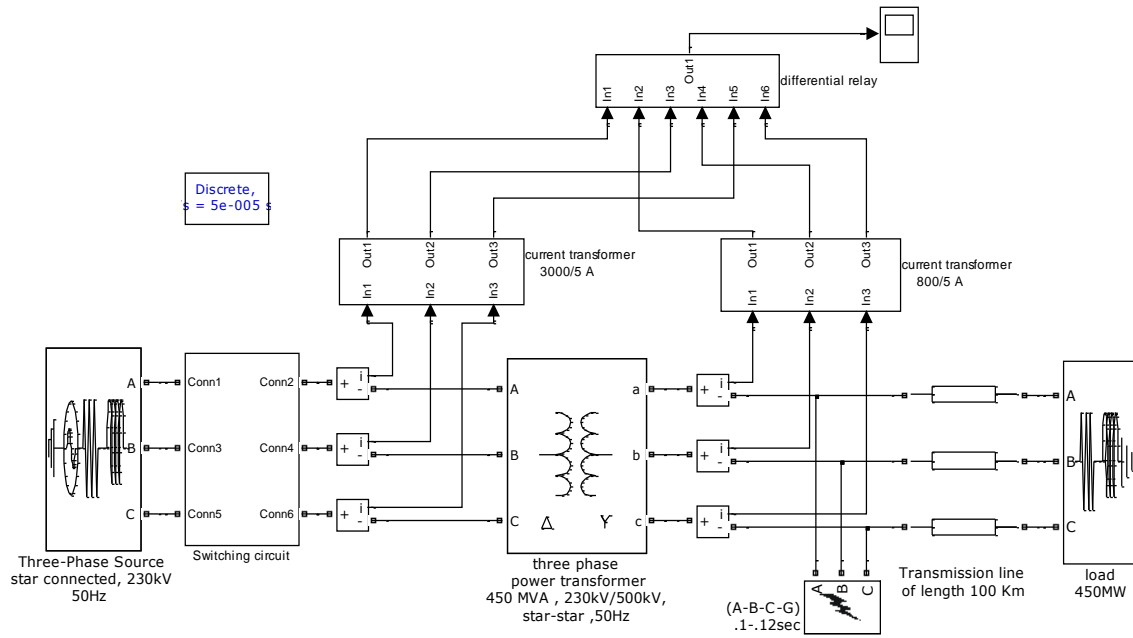Fig. A 2.2 Internal fault condition

External fault condition
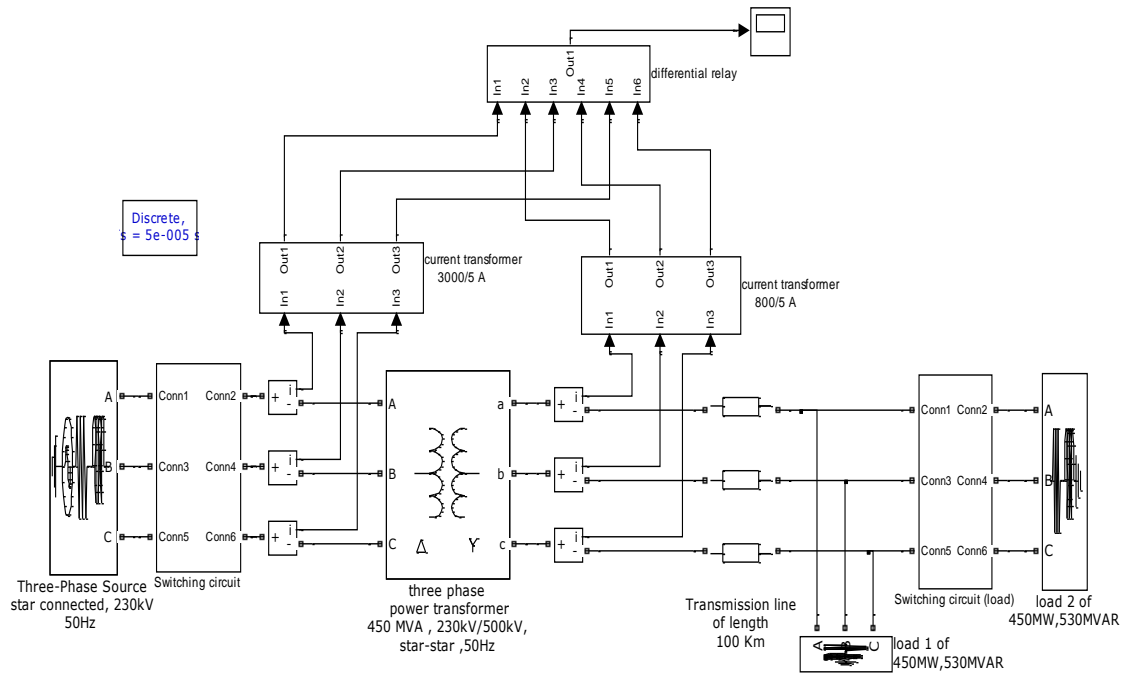

Fig. A 2.3 External fault

Over excitation condition

Fig. A 2.4 Over excitation condition

APPENDIX - 3

MATLAB CODES

Program to train ANN

```matlab
%A PROGRAM TO TRAIN NEURAL NETWORK
clear;clc;
IL=9;HL=16;OL=9;
n=0.2;m=0.9;
load q.mat
for i=1:36
    mx(i,:)=max(q(i,:));
     g(i,:)=q(i,:)/mx(i,:);
end
A=g;
Idata=A;
ts=zeros(36,9);
ts(1:4,1)=ones(4,1);        %normal
ts(5:8,2)=ones(4,1);       %inrush
ts(9:12,3)=ones(4,1);       %lg fault
ts(13:16,4)=ones(4,1);       %llg fault
ts(17:20,5)=ones(4,1);      % lllg fault
ts(21:24,6)=ones(4,1);       %ll fault
ts(25:28,7)=ones(4,1);       % lll fault
ts(29:32,8)=ones(4,1);        % external lllg fault
ts(33:36,9)=ones(4,1);          % over excitation
Wa=rand(IL,HL);
Wb=rand(HL,OL);
Wa0=zeros(size(Wa));
Wb0=zeros(size(Wb));
for j=1:20000
    for i=1:36
        IPattern=Idata(i,:);
         OPattern=ts(i,:);
        S1=IPattern*Wa;
      AF1=1./(1+exp(-S1));
        S2=AF1*Wb;
        AF2=1./(1+exp(-S2));
        Odata=AF2;
        Edata2=OPattern-Odata;
        e(i,:)=Edata2;
        % Back propagation of error
        delta2=Edata2.*(AF2.*(ones(size(AF2))-AF2));
        Edata1=delta2*Wb';
        Wb=Wb+n*(AF1'*delta2)+m*(Wb-Wb0);
        delta1=Edata1.*(AF1.*(ones(size(AF1))-AF1));
        Wa=Wa+n*(IPattern'*delta1)+m*(Wa-Wa0);
        Wb0=Wb;Wa0=Wa;
    end
    err(j,:)=sqrt(mean(e.*e));
    plot(err);
    dbt=err(:,5);
end
```

Wavelet analysis

```
%%%%%%%%%%%%%%%%%  WAVELET ANALYSIS   %%%%%%%%%%%%%%%%%%%%%%%
clc;clear all;
% WAVELET DECOMPOSITION
%file 1
%phase A
load ina1.mat
re1=(ina1(:,2));w1=re1(2000:2400);X1=w1;N1=5;
[c1,l1]=wavedec(X1,N1,'db6');
d1=detcoef(c1,l1,1);d2=detcoef(c1,l1,2);d3=detcoef(c1,l1,3);
d4=detcoef(c1,l1,4);d5=detcoef(c1,l1,5);
m1=mean(d1);s1=std(d1);n1=norm(d1);m2=mean(d2);s2=std(d2);
n2=norm(d2);m3=mean(d2);s3=std(d2);
n3=norm(d2);m4=mean(d2);s4=std(d2);n4=norm(d2);m5=mean(d2);s5=std(d2);
n5=norm(d2);
%file 2
%phase B
load inb1.mat
re2=(inb1(:,2));w2=re2(2000:2400);
X2=w2;N2=5;
[c2,l2]=wavedec(X2,N2,'db6');
d6=detcoef(c2,l2,1);d7=detcoef(c2,l2,2);d8=detcoef(c2,l2,3);
d9=detcoef(c2,l2,4);d10=detcoef(c2,l2,5);
m6=mean(d6);s6=std(d6);n6=norm(d6);m7=mean(d7);s7=std(d7);n7=norm(d7);
m8=mean(d8);s8=std(d8);n8=norm(d8);m9=mean(d9);s9=std(d9);n9=norm(d9);
m10=mean(d10);s10=std(d10);n10=norm(d10);
%file 3
%phase C
load inc1.mat
re3=(inc1(:,2));w3=re3(2000:2400);
X3=w3;N3=5;
[c3,l3]=wavedec(X3,N3,'db6');
d11=detcoef(c3,l3,1);d12=detcoef(c3,l3,2);d13=detcoef(c3,l3,3);
d14=detcoef(c3,l3,4);d15=detcoef(c3,l3,5);
m11=mean(d11);s11=std(d11);n11=norm(d11);m12=mean(d12);s12=std(d12);
n12=norm(d12);m13=mean(d13);s13=std(d13);n13=norm(d13);m14=mean(d14);
s14=std(d14);n14=norm(d14);m15=mean(d15);s15=std(d15);n15=norm(d15);
%file 4
%phase A
load ina2.mat
re4=(ina2(:,2));w4=re4(2000:2400);
X4=w4;N4=5;
[c4,l4]=wavedec(X4,N4,'db6');
d16=detcoef(c4,l4,1);d17=detcoef(c4,l4,2);d18=detcoef(c4,l4,3);
d19=detcoef(c4,l4,4);d20=detcoef(c4,l4,5);
m16=mean(d16);s16=std(d16);n16=norm(d16);m17=mean(d17);s17=std(d17);
n17=norm(d17);m18=mean(d18);s18=std(d18);n18=norm(d18);m19=mean(d19);
s19=std(d19);n19=norm(d19);m20=mean(d20);s20=std(d20);n20=norm(d20);
%file 5
%phase B
load inb2.mat
re5=(inb2(:,2));w5=re5(2000:2400);
X5=w5;N5=5;
[c5,l5]=wavedec(X5,N5,'db6');
d21=detcoef(c5,l5,1);d22=detcoef(c5,l5,2);d23=detcoef(c5,l5,3);
d24=detcoef(c5,l5,4);d25=detcoef(c5,l5,5);
m21=mean(d21);s21=std(d21);n21=norm(d21);m22=mean(d22);s22=std(d22);
n22=norm(d22);m23=mean(d23);s23=std(d23);n23=norm(d23);m24=mean(d24);
```

```matlab
s24=std(d24);n24=norm(d24);m25=mean(d25);s25=std(d25);n25=norm(d25);
%file 6
%phase C
load inc2.mat
re6=(inc2(:,2));w6=re6(2000:2400);
X6=w6;N6=5;
[c6,l6]=wavedec(X6,N6,'db6');
d26=detcoef(c6,l6,1);d27=detcoef(c6,l6,2);d28=detcoef(c6,l6,3);
d29=detcoef(c6,l6,4);d30=detcoef(c6,l6,5);
m26=mean(d26);s26=std(d26);n26=norm(d26);m27=mean(d27);s27=std(d27);
n27=norm(d27);m28=mean(d28);s28=std(d28);n28=norm(d28);m29=mean(d29);
s29=std(d29);n29=norm(d29);m30=mean(d30);s30=std(d30);n30=norm(d30);
%file 7
%phase A
load ina3.mat
re7=(ina3(:,2));w7=re7(2000:2400);
X7=w7;N7=5;
[c7,l7]=wavedec(X7,N7,'db6');
d31=detcoef(c7,l7,1);d32=detcoef(c7,l7,2);d33=detcoef(c7,l7,3);
d34=detcoef(c7,l7,4);d35=detcoef(c7,l7,5);
m31=mean(d31);s31=std(d31);n31=norm(d31);m32=mean(d32);s32=std(d32);
n32=norm(d32);m33=mean(d33);s33=std(d33);n33=norm(d33);m34=mean(d34);
s34=std(d34);n34=norm(d34);m35=mean(d35);s35=std(d35);n35=norm(d35);
%file 8
%phase B
load inb3.mat
re8=(inb3(:,2));w8=re8(2000:2400);
X8=w8;N8=5;
[c8,l8]=wavedec(X8,N8,'db6');
d36=detcoef(c8,l8,1);d37=detcoef(c8,l8,2);d38=detcoef(c8,l8,3);
d39=detcoef(c8,l8,4);d40=detcoef(c8,l8,5);
m36=mean(d36);s36=std(d36);n36=norm(d36);m37=mean(d37);s37=std(d37);
n37=norm(d37);m38=mean(d38);s38=std(d38);n38=norm(d38);m39=mean(d39);
s39=std(d39);n39=norm(d39);m40=mean(d40);s40=std(d40);n40=norm(d40);
%file 9
%phase C
load inc3.mat
re9=(inc3(:,2));w9=re9(2000:2400);
X9=w9;N9=5;
[c9,l9]=wavedec(X9,N9,'db6');
d41=detcoef(c9,l9,1);d42=detcoef(c9,l9,2);d43=detcoef(c9,l9,3);
d44=detcoef(c9,l9,4);d45=detcoef(c9,l9,5);
m41=mean(d41);s41=std(d41);n41=norm(d41);m42=mean(d42);s42=std(d42);
n42=norm(d42);m43=mean(d43);s43=std(d43);n43=norm(d43);m44=mean(d44);
s44=std(d44);n44=norm(d44);m45=mean(d45);s45=std(d45);n45=norm(d45);
%file 10
%phase A
load ina4.mat
re10=(ina4(:,2));w10=re10(2000:2400);
X10=w10;N10=5;
[c10,l10]=wavedec(X10,N10,'db6');
d46=detcoef(c10,l10,1);d47=detcoef(c10,l10,2);d48=detcoef(c10,l10,3);
d49=detcoef(c10,l10,4);d50=detcoef(c10,l10,5);
m46=mean(d46);s46=std(d46);n46=norm(d46);m47=mean(d47);s47=std(d47);
n47=norm(d47);m48=mean(d48);s48=std(d48);n48=norm(d48);m49=mean(d49);
s49=std(d49);n49=norm(d49);m50=mean(d50);s50=std(d50);n50=norm(d50);
%file 11
%phase B
load inb4.mat
re11=(inb4(:,2));
w11=re11(2000:2400);
```

```matlab
X11=w11;N11=5;
[c11,l11]=wavedec(X11,N11,'db6');
d51=detcoef(c11,l11,1);d52=detcoef(c11,l11,2);d53=detcoef(c11,l11,3);
d54=detcoef(c11,l11,4);d55=detcoef(c11,l11,5);
m51=mean(d51);s51=std(d51);n51=norm(d51);m52=mean(d52);s52=std(d52);
n52=norm(d52);m53=mean(d53);s53=std(d53);n53=norm(d53);m54=mean(d54);
s54=std(d54);n54=norm(d54);m55=mean(d55);s55=std(d55);n55=norm(d55);
%file 12
%phase C
load inc4.mat
re12=(inc4(:,2));w12=re12(2000:2400);
X12=w12;N12=5;
[c12,l12]=wavedec(X12,N12,'db6');
d56=detcoef(c12,l12,1);d57=detcoef(c12,l12,2);d58=detcoef(c12,l12,3);
d59=detcoef(c12,l12,4);d60=detcoef(c12,l12,5);
m56=mean(d56);s56=std(d56);n56=norm(d56);m57=mean(d57);s57=std(d57);
n57=norm(d57);m58=mean(d58);s58=std(d58);n58=norm(d58);m59=mean(d59);
s59=std(d59);n59=norm(d59);m60=mean(d60);s60=std(d60);n60=norm(d60);
% for detail 1 level
A=[m1 s1 n1 m6 s6 n6 m11 s11 n11;
 m16 s16 n16 m21 s21 n21 m26 s26 n26;
 m31 s31 n31 m36 s36 n36 m41 s41 n41;
 m46 s46 n46 m51 s51 n51 m56 s56 n56];
% for detail 2 level
B=[m2 s2 n2 m7 s7 n7 m12 s12 n12;
 m17 s17 n17 m22 s22 n22 m27 s27 n27;
 m32 s32 n32 m37 s37 n37 m42 s42 n42;
 m47 s47 n47 m52 s52 n52 m57 s57 n57];
% for detail 3 level
C=[m3 s3 n3 m8 s8 n8 m13 s13 n13;
 m18 s18 n18 m23 s23 n23 m28 s28 n28;
 m33 s33 n33 m38 s38 n38 m43 s43 n43;
 m48 s48 n48 m53 s53 n53 m58 s58 n58];
% for detail 4 level
D=[m4 s4 n4 m9 s9 n9 m14 s14 n14;
 m19 s19 n19 m24 s24 n24 m29 s29 n29;
 m34 s34 n34 m39 s39 n39 m44 s44 n44;
 m49 s49 n49 m54 s54 n54 m59 s59 n59];
% for detail 5 level
E=[m5 s5 n5 m10 s10 n10 m15 s15 n15;
 m20 s20 n20 m25 s25 n25 m30 s30 n30;
 m35 s35 n35 m40 s40 n40 m45 s45 n45;
 m50 s50 n50 m55 s55 n55 m60 s60 n60];
%%%%%%%%%%%%%%%%%%%%%%%%%%%%%%%%%%%%%%%%%%%%%%%%%%%%%%%%%%%%%%%%%%%%%%%%
```
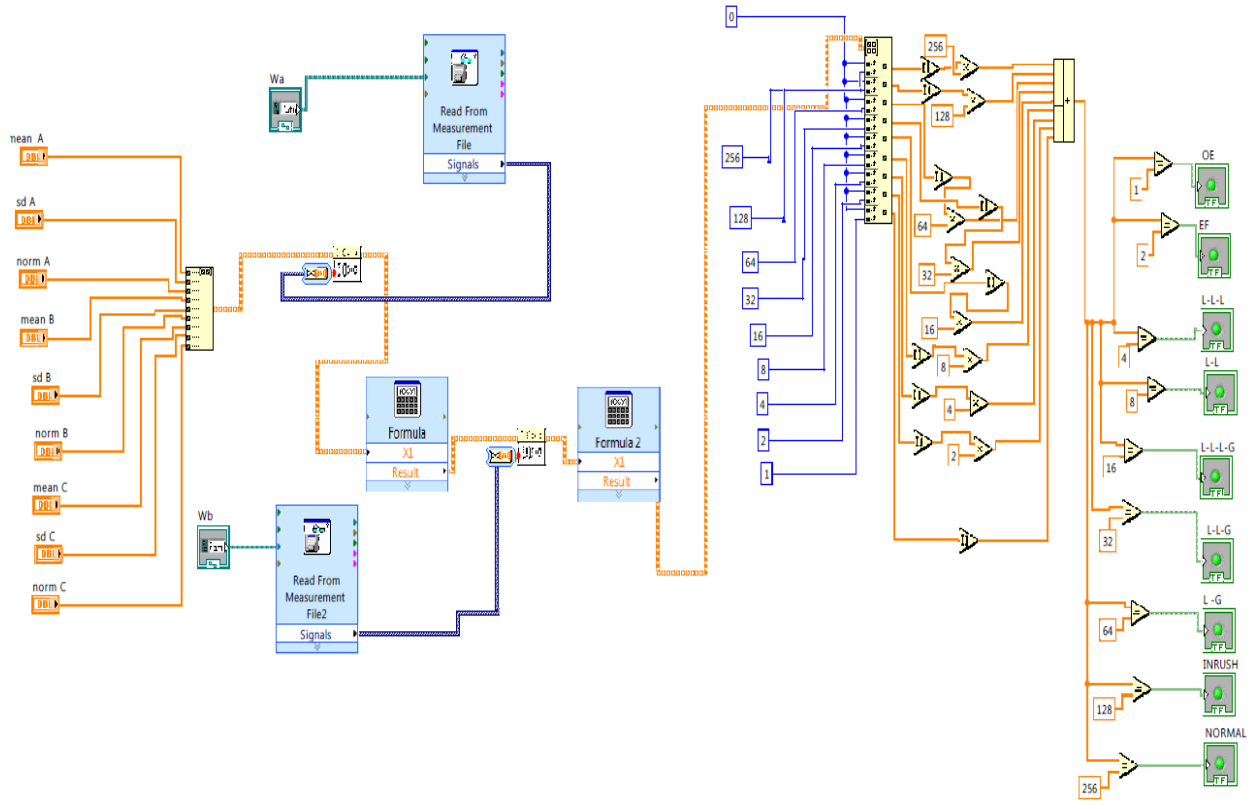
APPENDIX- 4

LabVIEW implementation of ANN

Fig A 4 LabVIEW implementation of ANN.